# Mid-Holocene sea-ice dynamics and climate in the northeastern Weddell Sea inferred from an Antarctic snow petrel stomach oil deposit

Mark A. Stevenson<sup>1a</sup>, Dominic A. Hodgson<sup>2,1</sup>, Michael J. Bentley<sup>1</sup>, Darren R. Gröcke<sup>3</sup>, Neil Tunstall<sup>1</sup>, Chris Longley<sup>1</sup>, Alice Graham<sup>1</sup>, Erin L. McClymont<sup>1</sup>

<sup>1</sup>Department of Geography, Durham University, Durham, DH1 3LE, United Kingdom

Correspondence to: Mark A. Stevenson (mark.stevenson@arch.ox.ac.uk)

Abstract. Understanding past variability in Antarctic sea ice is of critical importance to determine how it regulates global climate processes-and, biogeochemistry, and Southern Ocean marine ecosystems. Records of changes in Holocene sea-ice extent conditions in the Weddell Sea is are limited to a few marine sediment cores and inferences from continental ice cores. Here we present a novel record of sea- ice and climate from ~6700 \_ 20006390 to 1830 cal. yr BP based on accumulation rates and multi-proxy geochemical analyses of a snow petrel stomach-oil deposit from the Heimefrontfiella Range. Dronning Maud Land, East Antarctica. Three different sea-ice configurations are interpreted from the record. From 6700 6200 cal. yr BP there was a period of low sea ice cover and extensive polynyas associated with warmer temperatures and regional ice shelf retreat. From 6200 4700 cal. yr BP there was a gradual transition to more extensive sea ice configuration and a switch towards foraging in coastal polynyas at the retreating ice shelf front. Finally, between 4600 - 2000 cal. yr BP increased sea ice extent restricted access to foraging grounds which by ~6700 cal. yr BP resulted in abandonment of the nest.In the first interval, from 6390 to 5960 cal. yr BP, we see evidence of high productivity and inputs of krill, which suggests foraging both at the continental shelf edge in the MIZ and extending offshore over pelagic waters. We infer that the marginal ice zone (MIZ) lay within foraging range of Heimefronfjella. In the second interval, from 5960 to 4320 cal. yr BP, productivity remained 25 high, but there was a reduced influence of krill and likely more fish in the diet. This is consistent with foraging both over the continental shelf edge and offshore, supportive of the summer sea ice retreat reaching the shelf edge more frequently. Finally, in the final interval, between 4320 to 1830 cal. yr BP we infer very low productivity where increased sea-ice conditions restricted access to foraging grounds and open waters, with a less accessible MIZ resulting in a more dense sea-ice pack. Our results highlight how specific Holocene sea-ice configurations can be interpreted from the geochemical composition of snow petrel stomach-oil deposits, providing insight into the interactions between oceanographic forcing, climate change, ice-shelf extent and ecosystem adaptation. We also show, for the first time, the utility of phytol and cholesterol analysis for understandingtracking past avian diet.

<sup>&</sup>lt;sup>2</sup>British Antarctic Survey, Natural Environment Research Council, Cambridge, CB3 0ET, United Kingdom

<sup>&</sup>lt;sup>3</sup>Department of Earth Science, Durham University, Durham, DH1 3LE, United Kingdom

<sup>&</sup>lt;sup>a</sup>Present address: Oxford Radiocarbon Accelerator Unit (ORAU), School of Archaeology, University of Oxford, Dyson Perrins Building, South Parks Road, Oxford OX1 3QY, United Kingdom

#### 1 Introduction

35 Antarctic sea-ice extent isconditions are highly variable and closely coupled with continental, oceanic and atmospheric processes which both interact with and influence global climate (Brandon et al., 2010). Mechanistically, the formation of sea ice results in brine rejection which can directly contribute to the formation of Antarctic Bottom Water (AABW) (Crosta et al., 2022), helping drive ocean circulation, including the deep overturning cells (Ferrari et al., 2014) and supporting important circulation systems such as the Weddell Gyre (Vernet et al., 2019). UpwellingWithin the sea ice, upwelling can result in the 40 formation of open ocean polynyas within the sea ice, (areas of open water), whereas coastal polynyas are often driven by katabatic winds near the coast or at ice shelf fronts polynyas can form as a result of katabatic winds (Comiso and Gordon, 1987). These polynyas can support high levels of primary productivity in the ocean (Smith et al., 2010; Sarmiento et al., 2004; Arrigo et al., 2003).

Antarctic sea-ice records reveal pronounced declines in extent since 2016, associated with recent warming (Eayrs et al., 2021), with historic lows in 2023 and 2024 (Ionita, 2024; Purich and Doddridge, 2023; Gilbert and Holmes, 2024; Nsidc, 2024; Wang et al., 2024). Improved palaeoenvironmental reconstructions of Antarctic sea ice are vital to put instrumental observations (<50 years) into a longer-term context, with and projections of up to 67% decline by 2100 (Collins et al., 2013). Improved palaeoenvironmental reconstructions of Antarctic sea ice are vital to put these instrumental observations (<50 years) into a longer-term context. Such reconstructions provide a historical basis to understand the interactions between climate and sea-ice extentconditions, and interactions between sea ice and the extent of floating ice shelves and grounded ice.

Existing knowledge of Holocene Antarctic sea-ice evolution suggests there were three distinct phases, but these can be out of phase geographically due to regional responses and uncertainty associated with dating (Crosta et al., 2022). These eonsist of For coastal records, a cooler early Holocene between 11.5 ka to 8 ka BP (e.g. (Barbara et al., 2010; Etourneau Denis et al., 20132010; Peck et al., 2015; Mezgec et al., 2017; Nichols et al., 2019)), was followed by a warmer mid-Holocene (~7 to ~4–3 ka BP) with higher sea surface temperatures and longer ice-free summers (Crosta et al., 2022) and then a cooler late Holocene or 'neoglacial' phase ~5–3 to 1–0 ka BP marked by increased sea-ice extent as surface water temperatures reduced (Barbara et al., 2016; Taylor et al., 2001). However, records retrieved from beyond the coastal regions or those influenced by CDW (Circumpolar Deep Water) show an opposite pattern, with a warmer late Holocene (Bianchi and Gersonde, 2004; Nielsen et al., 2004; Etourneau et al., 2013; Vorrath et al., 2023), potentially in relation to the latitudinal and insolation and thermal gradients specifically associated with wind stress and upwelling (Denis et al., 2010). The integration of multiple records from the Atlantic sector of the Southern Ocean suggest there was some late Holocene cooling, driven by enhanced cold-water export from the Weddell Gyre as a cavity developed under the Ronne Filchner Ice Shelf, combined with a northward shift of the Southern Hemisphere westerly wind belt (Xiao et al., 2016). However, the changes within the Weddell Sea remain poorly understood and there is a lack of data to reconstruct past sea-ice evolution (Verleyen et al., 2011), particularly over the continental shelf.

To address this, we analysed a snow petrel (*Pagodroma nivea*) stomach-oil deposit, accumulated at <u>a nesting sitessite</u> in the <u>Heimefrontfjella region of Dronning Maud Land</u>, northeastern Weddell Sea-region. Such deposits have been previously demonstrated to record palaeoenvironmental information (McClymont et al., 2022; Berg et al., 2019; Ainley et al., 2006) by tracking the biochemical signature of changes in snow petrel diet, which is in turn related to environmental characteristics of their feeding grounds including sea-ice extent<sub>7</sub> and ocean productivity. Snow petrels have a close affinity with sea-ice-foraging zones during the breeding season (Delord et al., 2016; Ainley et al., 2006), feedings they feed in areas of intermediate sea-ice cover and switchingswitch between neritic (close to shore) and pelagic (offshore) feeding grounds (Ainley et al., 1998; Ainley et al., 1984).

Modern end-member studies have shown that specific prey species (e.g. krill, fish & squid) can be separated based on their fatty acid composition and can be used to infer different sea-ice conditions in the foraging area. For example, Antarctic (*Euphausia superba*) krill are high in C<sub>14:0</sub>, C<sub>16:0</sub> and C<sub>18:1</sub> fatty acids {(e.g. (Cripps et al., 1999)<del>†</del>), whereas squid are dominated by C<sub>16:0</sub> and fish by C<sub>18:0</sub> fatty acids {(Lewis, 1966); reviewed in McClymont et al. (2022)<del>†</del>. This). However, some fish can also be high in C<sub>18:1</sub>, especially C<sub>18:1(n-9)</sub> (e.g. the myctophid *Electrona carlsbergi*) (Connan et al., 2008). This broad framework allows us to distinguish between an Antarctic krill-rich diet, reflecting an offshore (pelagic) habitat, and a fish-rich diet, reflecting near-shore and continental shelf environments. Sea ice composition can be interpreted in terms of, based on the modern spatial distributiondistributions of fish (Ran et al., 2022; Liu et al., 2024; Freer et al., 2019), Antarctic krill (Mcbride et al., 2021) and cephalopod (mainly squid) (Xavier et al., 2016) species between coastal, shelf and offshore environments in the Southern Ocean and Weddell Sea. Stable isotopes in stomach—oils are also potentially excellent indicators of ecological baseline nutrient availability, trophic status (δ<sup>15</sup>N) and the productivity and location of past foraging habitats (δ<sup>13</sup>C) (McClymont et al., 2022; Ainley et al., 2006).

Here we analyse a well preserved snow petrel stomach oil deposit from the Heimefrontfjella region of Dronning Maud Land, East Antarctica to reconstruct changing Holocene sea ice and climate variability in the Weddell Sea. Using a radiocarbon dated age depth model, we analyse a range of organic geochemical biomarkers (including the first analyses of phytol and cholesterol in stomach oil deposits), bulk elemental chemistry and stable isotopes. Our record indicates three periods of distinctive Holocene climate and sea ice cover, which we compare with existing records of environmental changes in Antarctica and the Southern Ocean (Crosta et al., 2022).

Using a radiocarbon-based age-depth model, we analyse a range of organic geochemical biomarkers (including the first analyses of phytol and cholesterol in stomach oil deposits), bulk elemental chemistry and stable isotopes in the stomach oil deposit from Heimefrontfjella. These record three distinctive periods of Holocene climate and sea-ice cover, which we compare with existing records of environmental changes in Antarctica and the Southern Ocean.

#### 2 Materials and methods

2.1 Regional context

Formatted: Font: Bold

The Antarctic seasonal sea ice cycle is characterised by growth to maximum extent in September, followed by retreat to a minimum in February. Between the minimum and maximum sea-ice extents lies the Marginal Ice Zone (MIZ), characterised by sea-ice concentrations between 15-80%. In the northeastern Weddell Sea, the median sea-ice edge (15% sea-ice concentration) retreats rapidly with spring melt. In October/November, when the snow petrels start to return to their nesting sites, the sea-ice edge is located north of 60°S. Rapid sea-ice retreat through December brings the sea-ice edge to ~70°S by early January, spanning the snow petrel incubation phase, then retreats further westward until the minimum in February (Figure 1). The Weddell Sea gyre advects sea ice clockwise across the basin where it outflows in the northwest (Gupta et al., 2025). Sea ice tends to accumulate to the greatest extent in the south of the Weddell Sea due to this gyre (Hutchings et al., 2012).

The preferred foraging habitat of snow petrels has been observed to track the MIZ, where the presence of open waters within the sea ice facilitates access to prey (Wakefield et al., 2025). This foraging behaviour can see snow petrels foraging over and beyond the continental shelf, reaching ~700-1400 km from the nest site depending on the time of the breeding cycle and sea-ice extent (Honan et al., 2025). Based on regional tracking studies to the east, in Dronning Maud Land (Honan et al., 2025; Wakefield et al., 2025). three foraging options are available for snow petrels at Heimefrontfjella: (1) they head north to the MIZ lying to the south of the outer ice edge; (2) they north east to the Maud Rise, where an intermittent open-ocean polynya and earlier sea ice melt provides foraging habitat; (3) they forage in the MIZ closer to the continental shelf, which can be associated with coastal polynyas. Tracking studies show that the most likely scenario is that early in the breeding season snow petrels forage in association with the northern edge of the MIZ as the sea ice retreats (Wakefield et al., 2025). As the sea-ice edge retreats so does the foraging range, so that later in the season snow petrels are more likely to be found in coastal waters (Honan et al., 2025; Wakefield et al., 2025).

#### 2.2 Heimefrontfjella stomach oil deposit 3012MUM2-and its regional context

100

115

Stomach-oil deposit 3012MUM2 was collected in season 2014–15 from the Boysennuten nunatak in the Heimefrontfjella Range of East Antaretica (74° 34.14'S; 11° 15.02'W) (Fig. 1). The ~32 x 23 x 15 cm deposit with a maximum thickness depositof 19 cm had an irregular, mamillated outer surface, similar to previously sampled deposits from the wider region (McClymont et al., 2022). It was located immediately beneath a sheltered rock crevice, a typical habitat for nesting snow petrels, at an elevation of 1336 m above sea level (SI Fig.1a and 1b). It was kept in the dark and frozen at ~20 °C throughout the transportation processes to Durham University where sampling was carried out from 2021. The deposit was sliced using a circular saw while still frozen to preserve the internal millimetre-scale laminae which, when oriented, spanned a depth of ~19 cm, which was slightly smaller to along the maximum thickness of the deposit, due to the deposits mamillated structure and cutting on an axis to follow layering (SI Fig.1c). SamplingSub sampling was carried out at 2.5 mm resolution with 3.0 mm biopsy punches for organic geochemistry, isotopes and radiocarbon analyses. We selected a sampling line which represented the maximum accumulation rate and a continuous sequence through the stratigraphy; noting some heterogeneity either side of this line (Fig. 1 & SI Fig. 1c). A 19-cm long slice from the opposite face of the cut was mounted in plastic trunking for high-

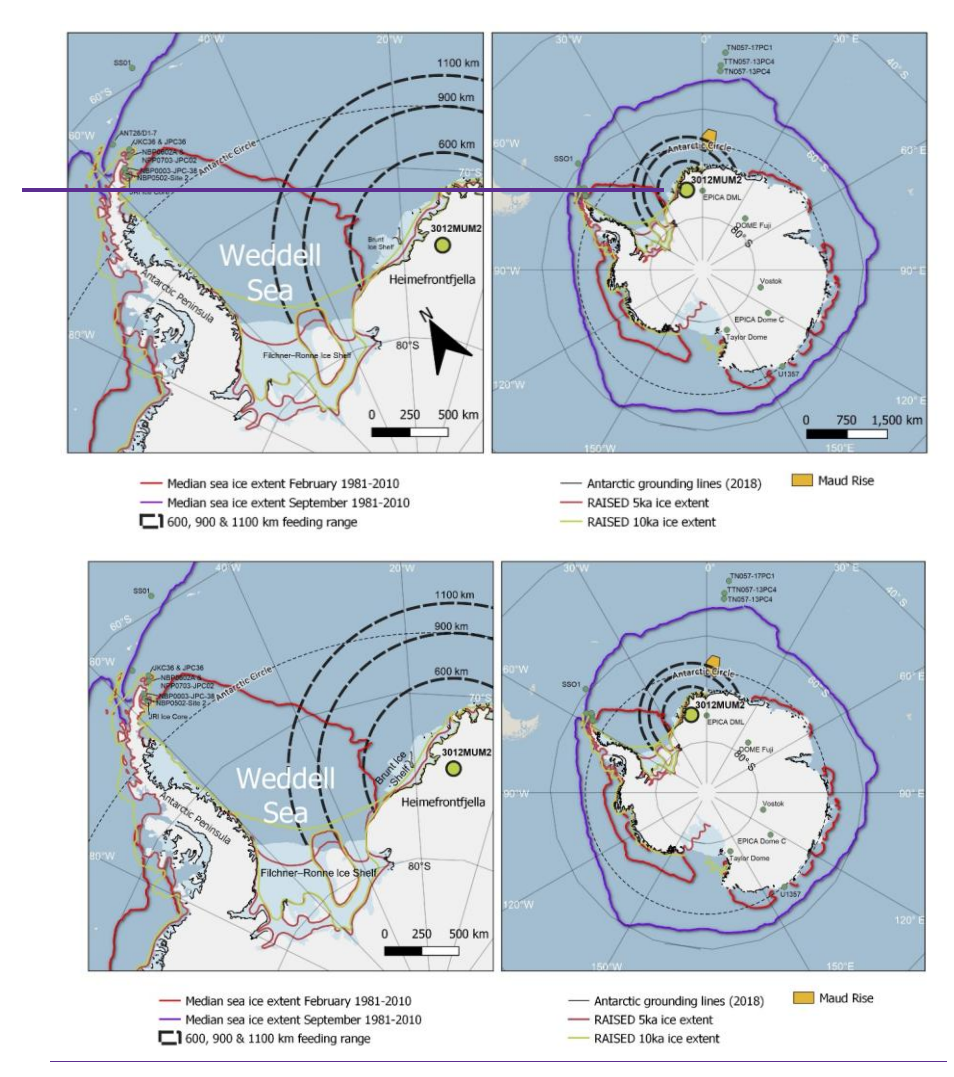


Figure 1: Location of Holocene snow petrel stomach oil record 3012MUM2, from Heimefrontfjella (74° 34.14'S; 11° 15.02'W; yellow circle) in the context of the Weddell Sea, and Antarctic Peninsula (left panel) and Antarctica and the Southern Ocean (right panel). Dashed

black lines indicate sectors within 600, 900 & 1100 km snow petrel foraging range from the stomach oil deposit. Also shown are median modern sea ice extentextents in February and September (Fetterer et al., 2017), RAISED grounded ice sheet extents at 5ka and 10ka (Bentley et al., 2014) and inferred modern Antarctic grounding lines (Rignot, 2022). Other locations and core sites mentioned in the text include: ice cores from EPICA DML (Masson-Delmotte et al., 2011); Dome Fuji (Masson-Delmotte et al., 2011); Pick Dome C (Masson-Delmotte et al., 2011); Vostok (Masson-Delmotte et al., 2011); Taylor Dome (Masson-Delmotte et al., 2011) and James Ross Island (JRI) (Mulvaney et al., 2012); marine sediment cores U1357 (Ashley et al., 2021); TTN057-13PC4 (Hodell et al., 2001); TN057-13PC4 (Divine et al., 2010; Nielsen et al., 2007); TN057-17PC1 (Divine et al., 2010; Nielsen et al., 2007); ANT28/DI-7 (Nie et al., 2022); NBP0003-JPC38 (Barbara et al., 2013); NBP0502-Site 2, Herbert Sound (Totten et al., 2015); NBP0602A & NPP0703-JPC02, Firth of Tay (Michalchuk et al., 2009; Majewski and Anderson, 2009); SS01 (Bak et al., 2007); and JKC36 & JPC36, Perseverance Drift (Kyrmanidou et al., 2018).

# 145 2.23 Radiocarbon analyses and age-depth modelling

160

An age-depth model for 3012MUM2 was constructed from twelve <sup>14</sup>C ages (Table 1). The top and bottom ages were sampled at 0 cm and 18.5 cm, immediately above and below the first geochemical samples (0.5 cm and 18.25 cm, respectively). Most of the radiocarbon ages were carried out by Beta Analytic (Miami, USA) using 14C-AMS via graphitization on untreated samples:, which were oxidised to CO<sub>2</sub> by combustion in O<sub>2</sub> and converted to graphite with Co powder as a catalyst. To assess for the effects of acid removal on 14C ages samples at 5.0 cm and 10.5 cm were repeat-sampled and analysed at SUERC (Scottish Universities Environmental Research Centre) Environmental Radiocarbon Laboratory by digestion in 1M HCL (hydrochloric acid) (at 80 °C, 2 hours), washed free of mineral acid with deionised water, dried and homogenised. Carbon was recovered from the residue as CO2 by heating with CuO in a sealed tube and converted to graphite by Fe/Zn reduction. Samples were then analysed by AMS at the Keck Carbon Cycle AMS Facility, University of California, Irvine, USA. For calibration of radiocarbon ages to calendar ages (Table 1) the MARINE20 radiocarbon age calibration (Heaton et al., 2020) was used, taking into account the regional marine reservoir effect using a of  $\Delta R = 670 \pm 50$  years, based on the marine reservoir effect measured at Hope Bay in the western Weddell Sea (Björck, 1991b). This approach has previously been applied to snow petrel stomach-oil deposits (McClymont et al., 2022). A Bayesian age depth model was then built in Bacon 2.3.9.1 (Blaauw and Christen, 2011). Following extensive testing, depth intervals (d.by) were set to 0.05, thickness to 1.2 (thick), accumulation rate mean (acc.mean) to 200, with minimum (d.min) and maximum (d.max) depth ranges set to 0 and 18.5 cm respectively. A Bayesian age-depth model was then built in OxCal v4.4 (Bronk Ramsey, 2009) using the default settings (applied with a general outlier model, except for paired dates where we used the SSimple outlier model). Our choice of a Bayesian approach to age-depth modelling means that the age uncertainties of all dates are considered for the entire age model. This means the final age model does not necessarily pass through the central median age of each date (if calibrated individually), but instead more accurately takes into account the entire profile (Blaauw and Christen, 2011; Blaauw et al., 2023).

Table 1: Radiocarbon dates including raw <sup>14</sup>C, F<sup>14</sup>C and Bayesian calibrated ages for the 3012MUM2 sequence, together with interpolated ages for top and base of samples used for biomarker/isotope sampling. Samples analysed by BETA Analytic (Florida) <sup>14</sup>C-AMS were prepared without acidification. Repeat analyses at 5 cm and 10.5 cm were prepared at SUERC Radiocarbon Laboratory using acidification and run for <sup>14</sup>C-AMS at UC Irvine Keck Carbon Cycle AMS]aboratory. A reservoir offset based on closest Holocene ΔR of 670 ± 50 years (Björck, 1991a) was used, eon-sistent with following previous studies (McClymont et al., 2022) and converted to calendar ages using the MARINE20 calibration (Heaton et al., 2020). All dates (<sup>14</sup>C and calibrated) rounded to nearest 10 calendar years for presentation, original measured dates are available at Pangaea (doi.pangaea.de/10.1594/PANGAEA.980519). The Bayesian model output is shown in Fig. 2.

Formatted: Italian (Italy)
Formatted: Italian (Italy)
Field Code Changed
Field Code Changed
Field Code Changed
Formatted: Italian (Italy)
Formatted: Italian (Italy)
Formatted: Italian (Italy)
Field Code Changed
Field Code Changed
Formatted: English (United Kingdom)
Formatted: French (France)
Formatted: French (France)
Y

Field Code Changed

Depth	AMS lab	Age (14C	±	<u>F<sup>14</sup>C</u>	Bayesian mo	delled calib	orated
(cm)	ID/ <i>deposit</i>	yr BP)	(14C		age using rba	eon <u>P sequer</u>	ice in
	position		yr		OxCal (cal. yr	BP). (see Fig	.2,)
	information		BP)		Median Min	Max	Min
0.0	Beta - 679228	2510	30	14590.7316	1134 <u>1260</u>	23031420	1060
0.5	Top of bioma	rker/isotope	N/A	N/A	<del>1983</del> <del>165</del> 4	<del>2407</del>	
	sampling						
1.0	Beta - 620905	3520	30	<del>2446</del> 0.6452	<del>1901</del> <u>2420</u>	<del>2926</del> 2670,	2210
3.5	Beta - 679229	4630	30	40020.5619	<del>3491</del> <u>3780</u>	4611,4000	3560
5.0	Beta 620906*	5030	30	45190.5346	4158 <u>4240</u>	<del>5119</del> 4420	4050
5.0	UCIAMS-	4958	35	45190.5394	41584240	<del>51194420</del>	4050
	276896*						
5.5	Beta - 620907	4990	30	46080.5373	42554280	<u>52034450</u>	4090
10.0	Beta - 620908	5520	30	<del>5251</del> 0.5030	4 <del>908</del> 4940	<del>5843</del> 5150	4770
10.5	Beta620909*	5610	30	53200.4974	4980 <u>4990</u>	<del>5922</del> 5200	4820
10.5	UCIAMS-	<del>5491</del> 5490	35	53200.5048	4980 <u>4990</u>	<del>5922</del> 5200	4820
	276897-						
13.5	Beta - 620910	5910	30	<del>5750</del> 0.4792	<del>5396</del> 5430	6348,5600	5250
17.0	Beta - 620911	6720	30	65250.4332	61216280	71286440	6100
18.25	Base of	N/A	N/A	6724	6332	7326	
	biomarker/isotope						
	sampling						
18.5	Beta - 679230	6840	30	6766 <u>0.4268</u>	6383 <u>6410</u>	7369 <u>6610</u>	6250

\*Bayesian P-Sequence model applies single age to paired date due to R\_Combine function in OxCal.

# 2.34 Bulk stable isotope analysis and organic matter elemental composition

StableCarbon and nitrogen stable isotope analysis was performed using a Costech ECS400 elemental analyser coupled to a Thermo Scientific Delta V Advantage isotope ratio mass spectrometer in the Stable Isotope Biogeochemistry Laboratory (SIBL) at Durham University. The method used is described in McClymont et al. (2022). Stable isotope analysis of carbon

Inserted Cells	
Formatted	
Formatted	
Formatted	
Formatted	
Deleted Cells	
Inserted Cells	
Formatted	
Inserted Cells	
Formatted	

Formatted
Formatted
Formatted
Formatted
Formatted

and nitrogen isResults are reported in standard delta ( $\delta$ ) notation in per mil ( $\infty$ ) relative to Vienna Pee Dee Belemnite (VPDB) and atmospheric nitrogen (AIR) respectively. The linear range for  $\delta^{13}$ C was between -46 % and +3 % and for  $\delta^{15}$ N between -4.5 % and +20.4 %, based on daily analysis of international (e.g. IAEA-600, IAEA-CH-3, IAEA-CH-6, IAEA-N-1, IAEA-N-2, NBS 19, USGS24, USGS40) and in-house standards, enabling a 2-standard-deviation analytical uncertainty of  $\pm 0.1$  % for international standards (replicated) and  $<\pm 0.2$  % on replicated samples. Total carbon (wt % C) and nitrogen (wt % N) were obtained simultaneously using an internal standard of glutamic acid (40.8 wt % C; 9.5 wt % N).

#### 2.45 Biomarker analyses

190

195

200

205

210

The biomarker sub-samples (0.02 - 0.05 g) were extracted in 4 mL dichloromethane (DCM):hexane (3:1) after addition of internal standards (nonadecane, heptadecanoic acid, 5α-androstane, 5α-androstanol) and then sonicated for 15 mins. Extracts were decanted and the procedure was repeated three more times. Extracts were combined and taken to dryness using rotary evaporation and N<sub>2</sub>. The entire sample was then saponified using 1 ml KOH (8%) in methanol (95%), heated for 1 h at 70 °C and left overnight. The neutral fraction was extracted with 3 x 3 ml hexane. The remaining sample was acidified to pH <3 using drops of 2M HCL, followed by extraction of fatty acids with hexane and evaporation to dryness with N<sub>2</sub>. Fatty acid methyl esters (FAMEs) were generated by methylating the fatty acid fraction using 3 mL methanol:HCL (95:5) heated for 12 h and left to cool. Samples were rinsed with 4M DCM-cleaned H<sub>2</sub>O and then FAMEs were extracted with at least three DCM:hexane rinses (4:1), before evaporation to dryness under N<sub>2</sub>. Neutral fractions were separated in up to four fractions using 4 cm deactivated silica (heated 140 °C for 16 h) columns in glass pipettes plugged with extracted cotton wool (silica pore size 60Å, 220-240 mesh particle size; 35-75 µm particle size (Sigma-Aldrich 60738-1KG)). Hexane was used to condition the columns (x3 column volumes) followed by injection of the sample dissolved in 500 µl DCM directly into the column. Elution order into separate fractions used three column volumes each of hexane, DCM, DCM:methanol (1:1) and methanol. All fractions were decanted and transferred into GC vials and evaporated to dryness using N2. Fraction F3 (DCM: Methanol methanol (1:1))), which recovered n-alcohols, phytol and sterols, was then further derivatized to trimethylsilyl esters prior to analysis using 50 µl DCM and 50 µl BSTFA (N,O-Bis(trimethylsilyl)trifluoroacetamide) (with 1% TMCS (chlorotrimethylsilane)) heated for 1 h at 70 °C and left overnight prior to analysis. Samples were evaporated to dryness and dissolved in hexane prior to analysis.

All extracts were analysed using a Thermo Trace 1310 gas chromatograph coupled to an ISQ LT single quadrupole mass spectrometer (GC-MS). FAMEs extracts were separated using a Restek FAMEWAX (crossbond polyethylene glycol) column (30 m x 0.25 mm x 0.25 mm x 0.25  $\mu$ m), similar to McClymont et al. (2022) but with some modifications. Briefly, samples were injected (0.8  $\mu$ l) into a programmable temperature vapouring (PTV) injector in CT Splitless mode with inlet temperature at 250 °C, carrier gas in constant flow and with helium carrier gas set to 1.5 mL min<sup>-1</sup> (split flow 15.0 mL/min; splitless time 1.5 min; purge flow 5.0 mL/min). GC oven temperature was set to 100 °C for 3 min followed by 2 °C/min to 230 °C; hold of 12 min. Prep-run timeout was 10 mins and equilibration time 0.5 min. MS settings included: transfer line, 230 °C; ion source temperature, 230 °C, mass range 38 to 600 m/z (every 0.5 s). Compounds were identified from their respective mass spectra

and retention times, with quantities calculated relative to the peak area of the internal standard heptadecanoic acid and an assumption of a 1:1 response (validated by comparison with Supelco 37 component FAME mix (CRM47885, Merck)).

Fraction F3 (previously eluted in DCM: Methanol (1:1)) was separated using a Restek Rxi-5ms (crossbond 5% diphenyl/95% dimethyl polysiloxane) column (60 m x 0.25 mm x 0.25  $\mu$ m). Similarly, samples were injected (0.8  $\mu$ l) into a programmable temperature vapouring (PTV) injector in CT split-less mode but at 280 °C inlet temperature, with helium carrier gas set to 2.3 mL min<sup>-1</sup> set in constant flow mode (split flow set to 23 mL/min; splitless time 1 min; septum purge flow 5.0 mL/min). GC oven temperature was set to 50 °C hold for 2 min followed by 10 °C/min to 200 °C; followed by a slower ramp of 3 °C/min to 300 °C and a hold of 20 min (prep run timeout was 10 min, equilibration time 0.5 min). MS settings included: transfer line, 310 °C; ion volume, 300 °C, mass range 50 to 550 m/z (every 0.5 s). Compounds were identified from their respective mass spectra and retention times, with quantities of trimethylsilyl esters (TMS) calculated relative to the peak area of the internal standard  $5\alpha$ -androstanol and an assumption of a 1:1 response (validated by identically derivatized standard mix which included cholesterol-TMS).

# 2.56 XRF analyses

215

220

230

XRF (X-ray fluorescence) analysis was carried out at Durham University, Department of Geography using a GEOTEK XRF Core Workstation (MSCL-XYZ) equipped with a rhodium source X-ray generator with a 10 mm cross-core slit width and a 1 mm downcore window. During operation the XRF scanner was set to analyse four different beam conditions, with a counting time of 10 seconds per beam. Beam conditions applied to the generator included: (1) no filter, 10 kV; (2) 25 µm silver filter, 20 kV; (3) 125 µm silver filter, 30 kV; (4) 625 µm copper filter, 50 kV. Detector measurement of photons ranged 2–35 keV. To pre-screen complex data, including removal of missing values and selecting elemental compositions from the most appropriate beam, the R 3.6.0 package 'tidyverse' (Wickham et al., 2019) was used to produce a master XRF dataset.

# 2.67 ICP-OES analysis

To determine local bedrock chemistry, a sample of rockTo determine local bedrock chemistry, a sample of gneissic granite rock (consistent with local geology (Juckes, 1972)) attached to deposit 3012MUM2 was soaked in ethanol to remove stomach-oil residue (repeated 3–4 times). It was then crushed using a fly press, freeze dried for 48 hours, and ground to a fine, homogenous powder using a ball mill. Organic matter was removed by adding 4 ml of 30% hydrogen peroxide to a ~0.5 g aliquot of rock. The sample was then digested for 4 hours in 16 ml of Aqua Regia using a DigiPREP digestion block, and subsequently diluted to 50 ml with deionised water and filtered at 0.45 µm. Elemental composition was determined using an Agilent Technologies 5100 Inductively Coupled Plasma Optical Emissions Spectrometer (ICP-OES).

### 2.78 Statistical and numerical analyses

Cluster analysis was carried out to highlight changes in geochemistry between neighbouring units in both inorganic (XRF) and organic (stable isotopes, TOC, C/N ratio and biomarkers) parameters down sample with depth. For each dataset (organic (Org  $\frac{1-3A-C}{2}$ ) and inorganic (XRF  $\frac{1-3A-C}{2}$ ), separately) a constrained hierarchical cluster analysis based on sample order was performed using the *rioja* package in *R* (Juggins, 2020) and compared with the A broken stick model of random zonesanalysis (Bennett, 1996) was used to identify the maximum number of statistically significant clusters.

Principal components analysis (PCA) was carried out in Canoco V.5.51 (Ter Braak and Smilauer, 2002) on log<sub>10</sub>-transformed and centred data: the inorganic (XRF) and organic (bulk organic geochemistry and biomarkers) parameters were treated separately. Input data for the organic PCA included bulk organics and biomarker concentrations, rather than fluxes (which included TOC normalized data and ratios). Input data for the inorganic PCA included XRF units in counts per second, rather than fluxes. As most XRF parameters had samples with counts <500 we chose to retain all parameters that had passed the pre-screening process (see section 2.5 XRF analyses). The lists of elements and compounds used in inorganic and organic PCA are shown in SI Tables 1 & 2.

#### 255 3 Results

#### 3.1 Stomach-oil deposit 3012MUM 2 age model

The stomach-oil deposit 3012MUM2 spans the interval of 1459 (1134–2303]260 (1060–1420) cal. yr BP at 0 cm and 6766 (6383–7369to 6410 (6250–6610) cal. yr BP at 18.5 cm (Table 1, reconstructed model, Fig. 2a). Biomarker When taking biomarker and isotope samples were not taken over as full a range aswe avoided the <sup>14</sup>C samples due to characteristic deposit plasticity at its margins and so we noteof the deposit, which were easily deformable. As a result, the oldest and youngest biomarker and isotope samples lie at 0.5 cm (1983 (1654–2407]1830 (1170–2530) cal. yr BP) and 18.25 cm (6724 (6332–73266390 (6210–6590) cal. yr BP) respectively in the Bayesian model, which we here summarise as ~2000or ~1800 to 67006400 cal. yr BP when rounded to closest 100 years. The accumulation rate based on the median Bayesian modelled age between radiocarbon dating depths varied between 10.18.6 and 70125.0 mm kyr-1 (Fig. 2b).

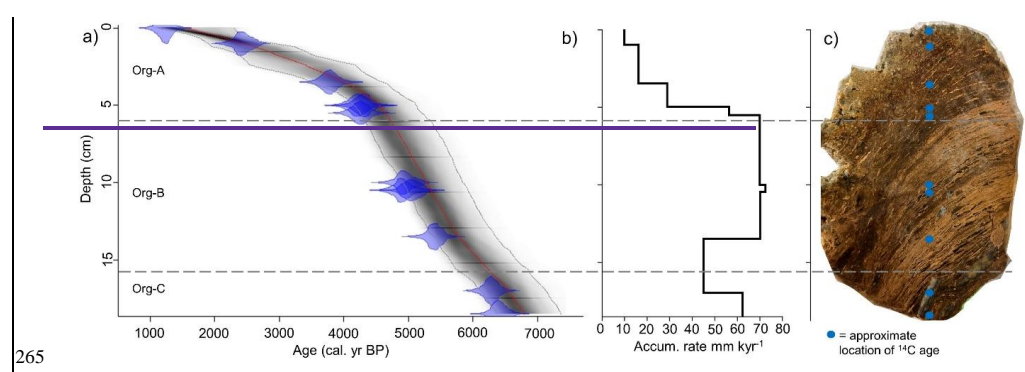


Figure 2: a) Bayesian <sup>14</sup>C AMS age depth model for stomach oil deposit 3012MUM2, generated in Bacon v2.3.9.1 (Blauw and Christen, 2011) applying a reservoir offset (\(\Delta R^{\text{Holocone}}\) (70 yr ± 50 years (McClymont et al., 2022)).

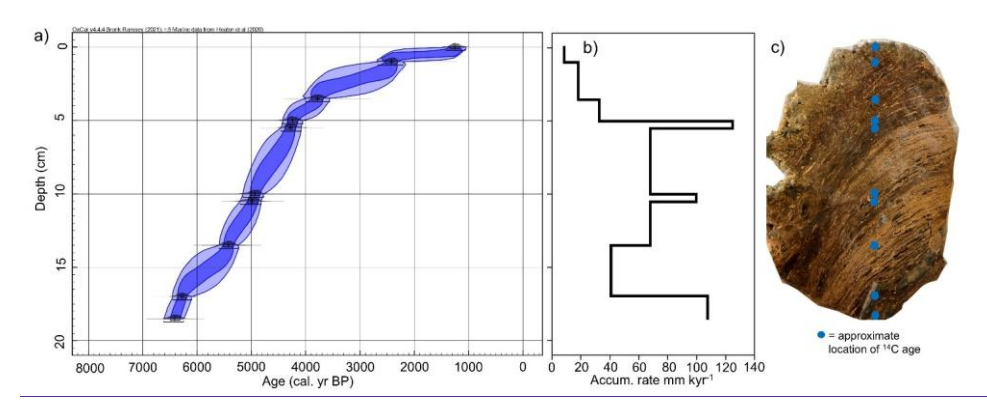


Figure 2: a) Bayesian  $^{14}\text{C-AMS}$  age-depth model for stomach oil deposit 3012MUM2, generated in OxCal (Bronk Ramsey, 2009) applying a reservoir offset ( $\Delta R^{\text{Holocene}}$  670  $\text{yr} \pm 50$  years (Björck, 1991a) calibrated to calendar ages using MARINE20 (Heaton et al., 2020). Dark blue ellipse indicates 68.3% range, light blue ellipse indicates 95.4% range. b) accumulation rate between age control points calculated from median ages in the Bayesian model in (a). c) photograph of stomach oil deposit 3012MUM2 after sectioning, complete with approximate location of  $^{14}\text{C}$  ages in blue dots. Constrained hierarchical cluster analysis was used to determine three significant clusters (Org A-C) using organic parameters in rioja (Juggins, 2020), compared with and the broken-stick model (Bennett, 1996).

### 275 3.2 Compositional changes in bulk organic matter and stable isotopes

Similar to previously measured snow petrel stomach-oil deposits [e.g. (McClymont et al., 2022; Berg et al., 2023; Hiller et al., 1988)|The 3012MUM2 samples were high in organic C (36.6 – 68.3% (mean 49.8%)) and total N (2.9 – 16.8% (mean 9.7%) (Fig. 3). The C:N<sub>atomic</sub> ratio varied between 3.4 and 20.8 (mean 7.5). Bulk  $\delta^{13}$ C had a narrow range from -31.0% to -29.5%,

with a mean of -30.3 % and a very small standard deviation (SD) of 0.3 % (Fig. 3), within the range of previous measurements of a Holocene deposit (Ainley et al., 2006). In contrast bulk  $\delta^{45}$ N had a wide range between 9.3 % and 19.1 % (mean 9.3 %, SD 1.6 %) (Fig. 3). In contrast bulk  $\delta^{15}$ N had a wide range between 9.3 % and 19.1 % (mean 12.2 %, SD 1.6 %) (Fig. 3).

#### 3.3 Compositional changes in biomarkers

280

285

300

Here and in the discussion, we present the majority of biomarkers as fluxes (Fig. 3). Given similar patterns with biomarker concentrations (SI. Fig. 2, 3 & 4) we consider the trends we have identified to be robust. The 3012MUM2 deposit samples likely comprised predominately—wax esters consistent with existing stomach oil studies (Imber, 1976; Lewis, 1966, 1969; Warham et al., 1976; Watts and Warham, 1976), although some may have already existed as free lipids. Once saponified and derivatised the extracts were rich in fatty acids (FA) and alcohols (FAle) (Fig. 3; SI Fig. 3). Diagnostically these fatty acids (FA) are commensurate with previous stomach oil and source end member studies which suggest a diet of krill (mainly C<sub>1440</sub> (FA), C<sub>1640</sub> (FA)), squid (C<sub>1640</sub> (FA)) and fish (C<sub>1640</sub> (FA), C<sub>1841</sub> (FA)) (Cripps et al., 1999; Lewis, 1966) summarised in McClymont et al. (2022), and contributions from free lipids. Once saponified and derivatised, the extracts were dominated by fatty acids (FA) and alcohols (FAlc) (Fig. 3; SI Fig. 3). In 3012MUM2, C<sub>1600</sub> was the most abundant fatty acid (mean 38.9% ± 8.8% SD), followed by C<sub>18:1(n-9)</sub> (FA) (mean 23.6% ± 10.9% SD), C<sub>14:0</sub> (FA) (mean 22.1% ± 5.2% SD), C<sub>18:0</sub> (FA) (mean 8.4% ± 2.1% SD) and C<sub>16:1</sub> (FA) (mean 7.1% ± 3.5% SD).

By flux and further explored in Berg et al. (2023). In 3012MUM2,  $C_{16:0}$  was the most abundant fatty acid (mean 38.9%  $\pm$  8.8% SD), followed by  $C_{18:1}$  (FA) (mean 23.6%  $\pm$  10.9% SD),  $C_{14:0}$  (FA) (mean 22.1%  $\pm$  5.2% SD),  $C_{18:0}$  (FA) (mean 8.4%  $\pm$  2.1% SD) and  $C_{16:1}$  (FA) (mean 7.1%  $\pm$  3.5% SD).

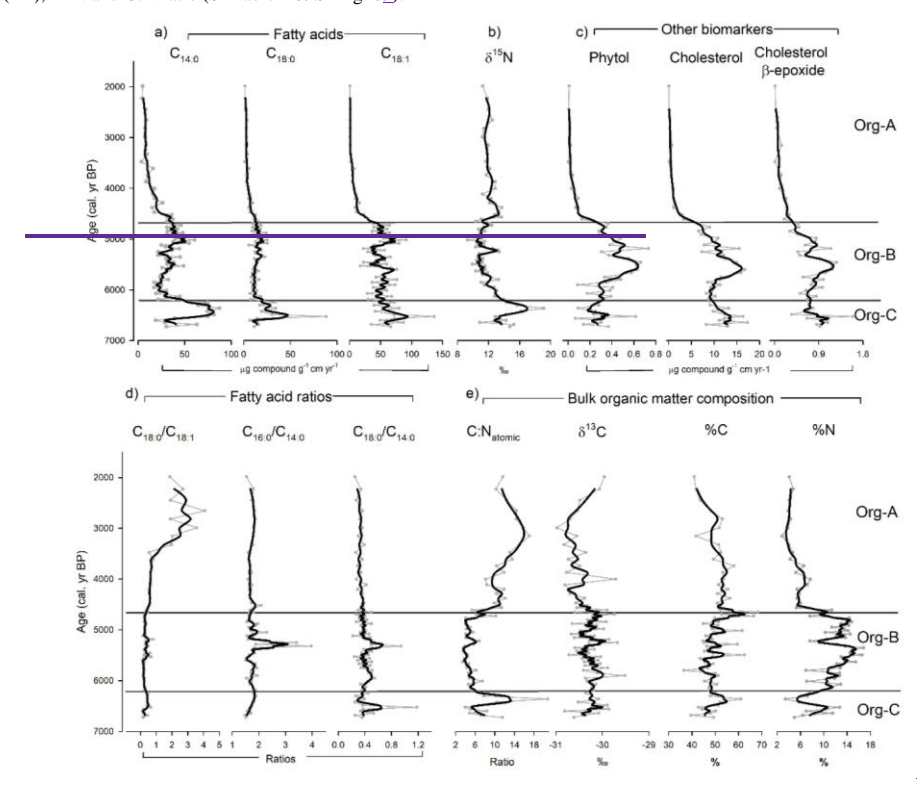
By concentration, FA were most abundant ( $C_{140}$ ,  $C_{160}$ ,  $C_{160}$ ,  $C_{180}$ ,  $C_{1800}$ ,  $C_{2000}$  &  $C_{2200}$  (FAlc) (total mean 4071.147.95 μg g<sup>-1</sup> TOCcm yr<sup>-1</sup>, SD 3210.5144.33 μg g<sup>-1</sup> TOCcm yr<sup>-1</sup>). The other compounds were less abundant, with cholesterol the highest (mean 757.7-19.95 μg g<sup>-1</sup> TOCcm yr<sup>-1</sup>, SD 429.6-17.47 μg g<sup>-1</sup> TOCcm yr<sup>-1</sup>) and phytol in lower concentrations (mean 24.7+10.31 μg g<sup>-1</sup> TOC; 14.0 cm yr<sup>-1</sup>; 0.22 μg g<sup>-1</sup> TOCcm yr<sup>-1</sup>). Phytol is formed from the ester-linked side chain of chlorophyll-a and can therefore primarily be considered a biomarker for phytoplankton (Rontani and Volkman, 2003). Cholesterol is a ubiquitous marker but in this context could be considered a krill marker (both Antarctic and ice krill), since it can account for more than 76% of total sterols in krill (Ju and Harvey, 2004) and is typically lower in concentration in fish- (e.g. cholesterol in *Dissostichus mawsoni* ranges 4.7-14.3% of total lipids (Clarke, 1984)). We also assessed the distributions of sterols (e.g 22-dehydrocholesterol), stanols (e.g. coprostanol) and cholesterol derivatives (e.g cholesterol  $\alpha/\beta$ -epoxide), with); cholesterol <u>was</u> the most abundant contributor (SI Fig. 4).

During saponification of the relevant wax esters, n-alkanols (FAlc) were also formed with saturated even chain lengths;  $C_{14:0}$  (FAlc) to  $C_{22:0}$  (FAlc) n-alcohols were the most abundant (SI Fig. 3). Amongst the n-alcohols  $C_{16:0}$  (FAlc) was the most abundant (mean 63%  $\pm$  2.9 % SD), followed by  $C_{14:0}$  (FAlc) (mean 22.4%  $\pm$  1.8 % SD) and  $C_{18:0}$  (FAlc) (mean 13.0%

Formatted: Superscript

 $\pm$  2.1% SD).  $C_{20:0}$  (FAlc) (mean 1.3%  $\pm$  0.4% SD) and  $C_{22:0}$  (FAlc) (mean 0.3%  $\pm$  0.1% SD) *n*-alcohols were relatively minor contributors.

Broadly, PC axis 1 (30% variance explained) for the organic geochemistry indicators had high positive loadings in C:N ratio and C<sub>18:0</sub>/C<sub>18:1(n-9)</sub> (FA), while PC axis 2 (24% variance explained) had strong positive loadings in C<sub>16:0</sub> (FA), C<sub>18:0</sub> (FA), δ<sup>15</sup>N and C:N ratio (SI Table 2 & SI Fig. 89).



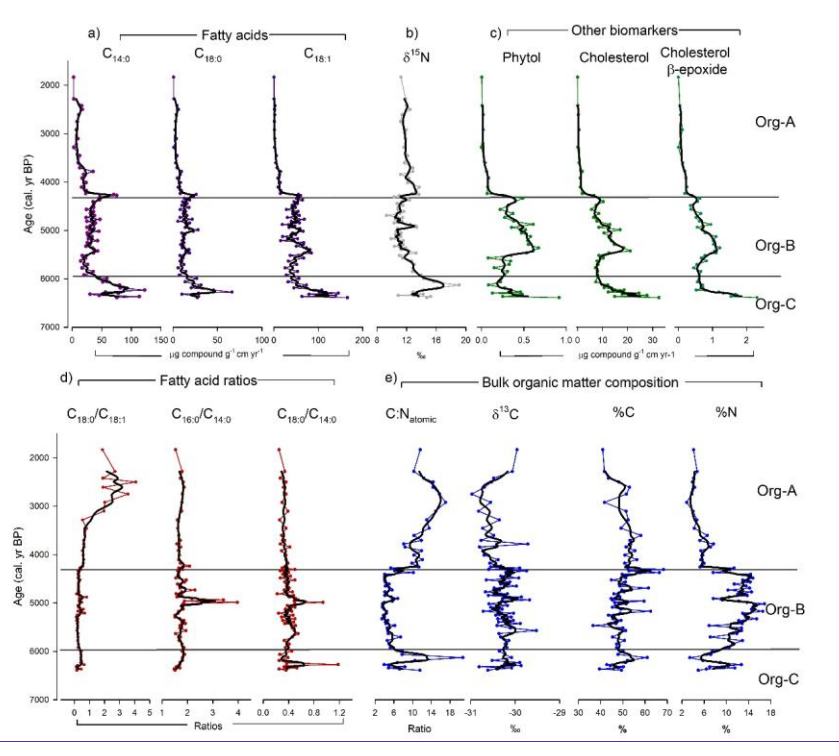


Figure 3: Organic parameters as fluxes and ratios measured in stomach oil deposit 3012MUM2, plotted against the age-depth model (Fig. 2). Smooth lines in bold are 3-point moving averages. Constrained hierarchical cluster analysis was used to determine three significant clusters (Org A-C) using organic parameters in rioja (Juggins, 2020), compared with the broken-stick model (Bennett, 1996). a) Fatty acid concentrations (C14-0, C18-0, C18-1/(1.00, C18-1/(1.00)); b) introgen stable isotopes ( $\delta^{15}N$ ); c) Other biomarkers (phytol & cholesterol); d) Fatty acid ratios (C18-0/C18-1/(1.00, C18-1/(1.00)); c) other measures of bulk organic matter composition (C:Natomic ratio,  $\delta^{13}C$ , %C and %N).

# 3.4 Changes in biomarkers through time

Cluster analysis identified three statistically significant organic zones (Org-A, B & C) which are used as a framework to discuss the changes in key biomarkers through time.3.4 Changes in biomarkers through time

Cluster analysis identified three statistically significant organic zones (Org-A, B & C) which are used as a framework to discuss the changes in key biomarkers through time.

Although clusters were identified from organic analyses, there were 8 zones of colour visible in 3012MUM2 (SI Fig. 1c). In terms of lithological units, zone Org-C closely matched with zone 8 (darkest layer, black/brown), with zones 4-7 matching

330 most closely with zone Org-B (lighter, yellowy/orange) and zones 1-3 matching with Org-A (medium-dark, grey brown to black brown).

### 3.4.1 Organic Zone - C (~6700 - 62006390 - 5960 cal. yr BP)

335

340

The base of thisthe deposit is marked by relatively high fatty acid (FA) fluxes: C<sub>14:0</sub> (FA), C<sub>18:0</sub> (FA) and C<sub>18:1(0:-9)</sub> (FA) increased to maxima around ~64006300 cal. yr BP and remained high todeclined by the top of the zone (62+65960 cal. yr BP) (Fig. 3). This is broadly coincident with a pulse of high δ<sup>15</sup>N (reaching ~20 %),%0, ~6100 cal. yr BP), which follows the trend in C<sub>14:0</sub> (FA) most closelybut is slightly offset (Fig. 3). Ratios of fatty acids C<sub>18:0</sub>/C<sub>18:1</sub>.(FA<sub>10-9</sub> and C<sub>16:0</sub>/C<sub>14:0</sub> (FA) remained low, with a pulse in C<sub>18:0</sub>/C<sub>14:0</sub> (FA) reaching a maximum at ~6300 cal. yr BP (Fig. 3). A peak of 60% C ~6100 cal. yr BP is reflected in the maximum C:N<sub>atomic</sub> ratio value of ~21 (Fig.6500 cal. yr BP (Fig. 3). A peak of 60% C ~6100 cal. yr BP is reflected in the maximum C:N<sub>atomic</sub> ratio value of ~21 (Fig. 3). δ<sup>13</sup>C fluctuated between ~29.9 % and ~30.8 %. Phytol and cholesterol were relatively high with phytol fluctuating between 0.06 and 0.6 μg g<sup>-1</sup> cm yr<sup>-1</sup> and cholesterol between 0.3 and 1.6 μg g<sup>-1</sup> cm yr<sup>-1</sup> (Fig. 3). All *n*-alkanols (FAlc) increased to higher concentrations around ~6200 cal. yr BP (SI Fig. 3). Most other biomarkers of sterols, stanols and cholesterol derivatives were generally high with phytol fluctuating between 0.06 and 0.6 μg g<sup>-1</sup> cm yr<sup>-1</sup> and cholesterol between 0.3 and 1.6 μg g<sup>-1</sup> cm yr<sup>-1</sup> and cholesterol between 0.3 and 1.6 μg g<sup>-1</sup> cm yr<sup>-1</sup> and cholesterol between 0.06 and 0.6 μg g<sup>-1</sup> cm yr<sup>-1</sup> and cholesterol between 0.3 and 1.6 μg g<sup>-1</sup> cm yr<sup>-1</sup> and cholesterol between 0.06 and 0.6 μg g<sup>-1</sup> cm yr<sup>-1</sup> and cholesterol between 0.3 and 1.6 μg g<sup>-1</sup> cm yr<sup>-1</sup> and cholesterol between 0.3 and 1.6 μg g<sup>-1</sup> cm yr<sup>-1</sup> and cholesterol between 0.3 and 1.6 μg g<sup>-1</sup> cm yr<sup>-1</sup> and cholesterol between 0.3 and 1.6 μg g<sup>-1</sup> cm yr<sup>-1</sup> and cholesterol between 0.3 and 0.6 μg g<sup>-1</sup> cm yr<sup>-1</sup> and cholesterol between 0.3 and 0.6 μg g<sup>-1</sup> cm yr<sup>-1</sup> and cholesterol between 0.3 and 0.6 μg g<sup>-1</sup> cm yr<sup>-1</sup> and cholesterol between 0.3 and 0.6 μg g<sup>-1</sup> cm yr<sup>-1</sup> and cholesterol b

# 3.4.2 Organic Zone – B (6200 – 4700(~5960 – 4320 cal. yr BP)

The transition to zone B (~5960 cal. vr BP) is marked by a rapid decrease in C<sub>14-0</sub> (FA), C<sub>16-0</sub> (FA) and C<sub>18-0</sub> (FA) fatty acid fluxes which thereafter remained broadly stable throughout the zone (Fig. 3; SI Fig. 2). 6200 cal. vr BP) is marked by a rapid decrease in C<sub>14-0</sub> (FA), C<sub>16-0</sub> (FA) and C<sub>18-0</sub> (FA) fatty acid fluxes which thereafter remained broadly stable throughout the zone (Fig. 3; SI Fig. 2). Zone Org-B has markedly lower δ<sup>15</sup>N (than zone Org-C, fluctuating between ~89 and 10 %).13 %. In contrast, the C<sub>16-1</sub> (FA) and C<sub>18-1(n-9)</sub> (FA) fatty acid concentrations decreased from around 5400 cal. vr BP to the top of zone Org-B, which is also observed in phytol and cholesterol from ~53005100 cal. vr BP (SI Fig. 2 & 3). Notably, the flux of fatty acids did not show a decline to the top of the zone, but remained fluctuating, with further peaks at ~5600 and 5000 cal. vr BP (Fig. 3). The major *n*-alkanols were markedly lower in zone Org-B compared to zone Org-C (SI Fig. 3), with a similar trend to lower values in C:N<sub>atomic</sub> ratio (Fig. 3). Notably, at ~49005200 cal. yr. BP there iswas a short-lived unusual interval of high δ<sup>15</sup>N, high C<sub>160</sub>/C<sub>14:0</sub> (FA), C<sub>18:0</sub>/C<sub>14:0</sub> (FA) and a small increase in C:N ratio (Fig. 3). Both δ<sup>13</sup>C (fluctuating ~ 30.7% to ~29.5%) and %C (fluctuating ~ 36.6 % to 66 %) were 3). Organic carbon composition was variable at this time (in zone Org-Ofg-C) and between ~36.6 % to 66 % for %C (Fig. 3). Fig. 3). Other biomarkers of sterols, stanols and cholesterol derivatives were generally high at the bottom of this-zone (62000rg-B (~5960 cal. yr BP),

Formatted: Subscript

typically decreasing by the top (~ 47004320 cal. yr BP) (SI Fig. 4). Organic PC1 remains low ~600 cal. yr BP, increasing slightly by the top of the zone (~4700 cal. yr BP), while PC2 is markedly lower throughout compared with zone C (SI Fig. 2).

# 3.4.3 Organic Zone - A (4700 - 2000(~4320 - 1830 cal. yr BP)

For most biomarkers zone  $\underline{Org}$ -A is a relatively stable period, with fluxes and concentrations of  $C_{14:0}$  (FA),  $C_{18:0}$  (FA) and  $C_{18:1(\underline{n}.9)}$  (FA) remaining low, broadly similar to the previous zone  $\underline{B}$ - and  $\underline{Org}$ -B. The fatty acid ratios  $\underline{C}_{16:0}/C_{14:0}$  (FA) and  $C_{18:0}/C_{14:0}$  (FA) are stable throughout (Fig. 3; SI Fig. 2 & 3). Between 42504000 and 45504320 cal. yr BP,  $\delta^{15}N$  was slightly higher (reaching 13.7 %) before decreasing towards the top of the deposit (Fig. 3).  $C_{14:0}$  (FAlc),  $C_{16:0}$  (FAlc) and  $C_{18:0}$  (F

#### 3.5 Inorganic composition (XRF)

#### 3.5 Inorganic composition (XRF)

390

Cluster analysis identified three major XRF clusters: XRF-C (6766 49046390-4570 cal. yr BP); XRF-B (4904 44964570-4180 cal. yr BP); XRF-A (4496-19834180-1830 cal. yr BP). Zone XRF-C broadly coincides with organic zone Org-C and B, with XRF-B aligning (although slightly offset) with the uppermost part of organic-zone Org-B. Zones XRF-A and organic zone Org-A are broadly aligned.

Based on XRF mean counts per second (CPScps) the largest elemental contributors to stomach-oil deposit 3012MUM2 were Cl, Ca, Fe, S, K, Br and P. Elevated Fe, Al, Mg and Ca in the rock specimen taken from 3012MUM2 (SI. Table 3) suggest that these elements have a locally-derived erosional contribution. Other elements potentially in part may derive from windblown particulates (Cl, S, Br and P) (Fig. 4, SI. Fig 5 & 6). Cu was also present which is known to be a key Antarctic krill marker as a Cu backbone structure is found in hemocyanin (Bridges, 1983).

Key XRF-derived inorganic compositions <u>normalised to accumulation rate</u> are presented in Fig. 4. Fe reflects a group of elements with high contributions to PC 1 (reflecting 28% of variance (SI Table 1; SI Fig. 9)) which 4. Fluxes are characterised by a <u>peak-higher variability</u> in XRF-C ~6500with <u>peaks in multiple elements at ~6300</u> cal. yr BP, followed by declines to ~6000~5300-4900 cal. yr BP. Values then gradually increase to a further <u>peak ~4000 cal.</u> yr BP and remain stable

Formatted: English (United Kingdom)

Formatted: English (United Kingdom)

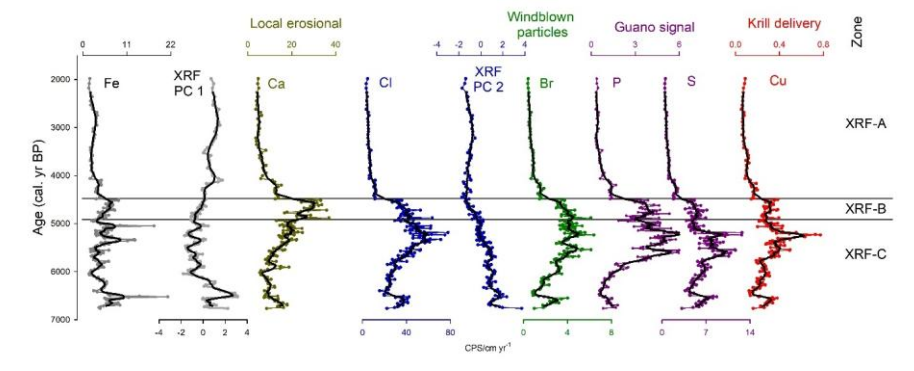
toat the top of the core. We posit Ca as an element driven by local erosion which has some similarities to PC1 but is marked by elevated values within zone (~4570 cal. yr BP). In XRF-B and an overall decline in XRF-Avalues reach a peak at ~4300 cal. yr BP. Elemental fluxes are lower and relatively stable in XRF-A, with a small peak in some elements such as Fe ~2400 cal. yr BP.

395

400

410

Cl reflects a group of compounds with high contributions to PC 2 (reflecting 22% of variance. PC2 is characterised by declines in XRF B to minimum values at the start of XRF A. Changes in PC 2 primarily reflect positive loadings in S and Cl (SI Table 1; SI Fig. 9) but negative loadings from elements which are commonly associated with seabirds (e.g. P, Zn, Sr, Ni), including Cu (Shatova et al., 2016; Shatova et al., 2017; Castro et al., 2021; Sparaventi et al., 2021) which supports our interpretation of an Antarctic krill marker. Broadly elevated Cu in organic zone B (with elevated C<sub>14-0</sub> FA and cholesterol) and low values for both in organic zone A support this interpretation, but we note that only Cu and cholesterol show comparable patterns in organic zone C. Cholesterol also tends to be a major component of guano (Cheng et al., 2016). We posit P and S as indicative of bird guano (Tatur et al., 1997; Roberts et al., 2017; Sun et al., 2000; Liu et al., 2005) and so likely to reflect prey, while Br has the potential to be windblown (Hughes et al., 2012). The relationship between nitrogen and minerogenic elements suggests some N has a guano origin given negative relationship between C:N and other elements (Cl, P, S) (SI Fig. 7) consistent with other studies (Berg et al., 2019; Hiller et al., 1988), but in contrast with a record from Marine Isotope Stage 3 (McClymont et al., 2022). A positive correlation between P and N also support a guano signal for these elements (SI Fig. 8). Bedrock contamination is unlikely given local gneiss bedrock (SI Table 3).



Based on the PCA of counts per second data, PC1 reflected 28% of the variance (SI Table 1; SI Fig. 10) and included Si, Ba Al and Fe, which tend to peak around ~6300 cal. yr BP in zone XRF-C (SI Fig. 5). PC2 reflected 22% of variance (SI Table 1; SI Fig. 10), and included S, Cl, Br, P and Cu, which shift towards lower values and lower variability in XRF-A (Fig. 4).

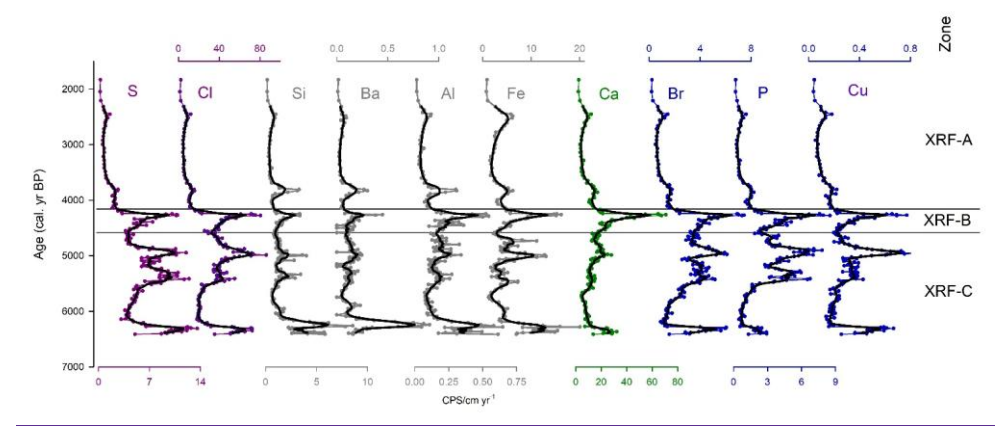


Figure 4: Key inorganic elements measured in stomach-oil deposit 3012MUM2, lottedplotted as qualitative counts per second (cps) normalised to accumulation rate, to approximate element fluxes against the age-depth model (Fig. 2). Elements includes include S, Cl, Si, Ba, Al, Fe, XRF-PC1, Ca, Cl, XRF-PC2, Br, P & Sand Cu. Plots are coloured according to PCA axes and our environmental interpretations: grey – positive secresgroupings on the PCA\_Black lines indicate 7-point moving averages. Cluster boundaries (XRF-A, B & C) and XRF PCA are uniquely calculated from entire XRF dataset (Figure SI Fig. 3).

# 4 Discussion

415

420

PC axis 1, blue = positive scores on PC axis 2, teal = local erosional, green = windblown particles, guano signal = purple & red = potential krill delivery, Black lines indicate 7-point moving averages. Cluster boundaries (XRF-A, B & C) and XRF PCA are uniquely calculated from entire XRF dataset (Figure SI Fig. 3).

# 425 4 Discussion

We found pronounced variations in geochemical proxies in stomach-oil deposit 3012MUM2 spanning much of the Holocene [--6724-1983 cal. yr BP (Bayesian modelled median age range)]. Given the dependence of snow petrel dietary composition on environmental showing snow petrel diet was responding to changes in sea-ice conditions this indicates that the Weddell Sea changed markedly through the Holocene in terms of sea ice extent and distribution, and ocean productivity and climate. These-related to changes are a result of the interactions between water mass upwelling, solar forcing, wind strength (including position of southern westerlies) and the moderating effect of expanding or contracting ice sheets (Denis et al., 2010; Hillenbrand et al., 2017), in ice sheet extent and climate. In this Discussion we first outline the rationale and caveats in our proxy interpretations, then explain the links between diet changes and sea ice environments through time.

#### 4.1 Role of ice shelf retreat on the accessibility of foraging areas—Proxy interpretations

In the Weddell Sea region, deglacial ice sheet thinning and retreat continued after ~8 ka High levels of organic C and N in 3012MUM2 were similar to previously measured snow petrel stomach oil deposits (e.g. (NicholsMcClymont et al., 2019; Johnson 2022; Berg et al., 2019 2023; Hiller et al., 1988)), while bulk δ<sup>13</sup>C values were within the range of previous measurements of a Holocene deposit (Ainley et al., 2006). The fatty acid (FA) distributions found in the stomach oils are commensurate with previous stomach-oil and source end-member studies which suggest a diet of krill (mainly C14:0 (FA), C16:0 440 (FA)), squid (C<sub>16:0</sub> (FA)) and fish (C<sub>16:0</sub> (FA), C<sub>18:1(n-9)</sub> (FA)) (Cripps et al., 1999; Lewis, 1966) as summarised in McClymont et al. (2022) and further explored in Berg et al. (2023)., whereby retreat of the Filchner and Ronne Ice Shelf was known to have been completed by 7.7.44C corrected kyrs BP on the inner shelf (Hillenbrand et al., 2017), corroborated by ice core sodium analyses (Grieman et al., 2024). Additionally Brunt Ice Shelf geophysical investigations supports the general picture of sustained retreat until at least 8351 cal. yr BP (Hodgson et al., 2018). Maintenance of the ice fronts in a retreat scenario from 445 the start of the record is consistent with our evidence of increased availability of productive foraging habitat. More widely, the transition to cooler temperatures was probably characterised by mid-Holocene ice shelf cavity expansion, which led to cooling of surface waters and expansion of sea ice, which in turn slowed basal melting at the ice sheet margin (Ashley et al., 2021). While some FAs are labile and susceptible to degradation, particularly unsaturated FAs (Stefanova and Disnar, 2000), the similar profiles shown by C<sub>14:0</sub> and C<sub>18:0</sub> FA with C<sub>18:1(n-9)</sub> FA suggests that changes in diet, not preservation, is the main driver 450 for the latter FA (Fig. 3).

In the PCA biplots for the XRF analysis (SI Table 1 & Fig. 10) negative loadings from elements which are commonly associated with seabirds (e.g. P, Zn, Sr, Ni), including Cu (Shatova et al., 2016; Shatova et al., 2017; Castro et al., 2021; Sparaventi et al., 2021) support our interpretation of dietary sources to the deposit (Duda et al., 2021). In contrast, the positive loading of Fe, Al, Si and Ca on PC1 aligns with the main elements measured in the rock specimen taken from 3012MUM2 (SI. Table 3), which reflects the local gneissic granite bedrock (Juckes, 1972). These elements are interpreted to reflect locally-derived, probably bedrock, erosional contribution. Cu was also present in 3012MUM2, which is known to be a key Antarctic krill marker as a Cu backbone structure is found in hemocyanin (Bridges, 1983) and has been observed in previous snow petrel deposits to be associated with Antarctic krill (McClymont et al., 2022). Broadly elevated Cu in zone Org-B with elevated C<sub>14:0</sub> FA and cholesterol (Fig. 3) also supports an Antarctic krill source for these components.

A wide range of  $\delta^{15}N$  values is recorded, which could reflect environmental change (e.g. changing circulation, degradation) or dietary change (e.g. baseline values in phytoplankton, trophic level). Past variations in the  $\delta^{15}N$  of circumpolar deep water (CDW) which upwells to the sea surface can contribute to high  $\delta^{15}N$  (Kemeny et al., 2018), but it is so far unknown if this occurred during the timescale of our deposit between 6390 and 1830 cal. yr BP (as opposed to glacial-interglacial timescales). Fragmented coral  $\delta^{15}N$  records of upper CDW indicate mid- to late Holocene values spanning ~7-11‰ (Chen et al., 2023) but without the resolution to compare shorter-term changes with the variations we observed in 3012MUM2. Diatombound records of baseline  $\delta^{15}N$  show a long-term decline through the Holocene as nutrient availability has increased (e.g. (Ai

460

465

et al., 2020; Studer et al., 2018)), which aligns in part with our overall trend. Previous work has cautioned that guano could contribute to stomach-oil deposits (Berg et al., 2019), which would also elevate  $\delta^{15}N$  (e.g. (Wainright et al., 1998; Bokhorst et al., 2007)). Finally, weathering would also elevate  $\delta^{15}N$  values due to microbial biosynthetic pathways causing <sup>14</sup>C release by (Macko and Estep, 1984). However, we only identified minor contributions from microbial fatty acids in 3012MUM2 to support this interpretation. In our discussion below, we focus on the environmental and dietary information provided by  $\delta^{15}N$  in combination with other proxy indicators.

We focus mainly on organic compounds for interpretation of palaeoclimate because dietary lipids and organic isotopes reflect the main snow petrel dietary sources which can, in turn, provide secondary information on sea ice distribution (e.g. (McClymont et al., 2022)). In particular, we focus on  $C_{14:0}$  (FA) as an indicator of past Antarctic krill contributions to the diet,  $C_{18:0}$  (FA) for fish,  $C_{18:1(n-9)}$  (FA) for mainly fish, bulk  $\delta^{15}$ N as primarily an indicator of trophic status and productivity, and phytol as an indicator of past productivity. In terms of past ice configurations, we interpret a diet with more Antarctic krill and high productivity as recording snow petrels feeding in the open ocean (within the MIZ or the open ocean) (e.g. zone Org-C). Zones of higher productivity with reduced Antarctic krill contributions are inferred to represent enhanced snow petrel feeding closer to shore, in neritic zones, either due to a more proximal MIZ or in coastal polynyas along the Antarctic ice sheet margin (e.g. zone Org-B). While zones with lower productivity and accumulation rates reflect sea ice expansion, a less accessible MIZ and a more dense ice pack (e.g. zone Org-A).

# 4.2 Interpreting changes in sea ice in mid-Holocene stomach-oil deposits

495

By the start of the 3012MUM2 record at ~6400 cal. yr BP, the Filchner and Ronne Ice Shelf had reached its modern position (Nichols et al., 2019; Johnson et al., 2019; Hillenbrand et al., 2017; Grieman et al., 2024). In other parts of Antarctica, cooling of the surface ocean and freshening of shelf surface waters since the middle-Holocene (Ashley et al., 2021) led to increased sea-ice concentrations and sea-ice duration over the continental shelf (Crosta et al., 2008; Mezgec et al., 2017; Johnson et al., 2021). Further offshore, sea ice became less extensive since ~6500 cal. yr BP (Nielsen et al., 2004; Xiao et al., 2016), reflecting shifts in the latitudinal insolation and thermal gradients (Denis et al., 2010) as well as the multi-centennial expression of climate modes, such as ENSO (El Niño-Southern Oscillation) (Crosta et al., 2021). For the wider southern ocean, exemplified in East Antarctica, after 4500 cal. yr BP although sea ice and turbulence persisted in locations proximal to the ice shelf, it did not increase further offshore due to northward transport of subpolar surface waters as a response to southern Westerlies reinforcement (Denis et al., 2010).

The evolution of Holocene sea ice has been separated into three distinct phases around Antarctica (Early Holocene \* 11.5 to \* 8 ka BP; mid-Holocene \* 7 to \* 4-3 ka BP; the late Holocene \* 5-3 to 1-0 ka BP), with the phasing of these periods differing depending on regional response to long-term forcing (Crosta et al., 2022). Despite this wider knowledge there is an absence of any paleoenvironmental reconstructions of sea ice for the Holocene within the Weddell Sea region. Here we explore how each of the three statistically significant geochemical zones in the stomach oil deposit align with the timing or direction of the environmental shifts recorded by Crosta et al. (2022) and similar studies elsewhere in Antarctica.

Formatted: Indent: First line: 1.27 cm

510

#### 4.2.1 Zone Org-C (6390-5960 cal. vr BP)

Between 6390-5960 cal. yr BP we infer that the snow petrels at Heimefronfjella had a mixed diet which reflected access to areas of high productivity similar to today, with a MIZ situated in pelagic waters but with the potential for foraging over the continental shelf when the MIZ was situated closer to the coast. This interpretation is based on geochemical evidence of a diet sporadically high in either Antarctic krill (Euphausia superba) (evidenced by FA C<sub>14:0</sub>, Cu: pelagic waters) or fish (evidenced by  $C_{18:0}$  (FA): continental shelf waters). While we are unable to constrain sea-ice extent precisely, we interpret the high but variable snow petrel stomach oil accumulation rates to reflect repeated nest occupation from an accessible foraging habitat. The MIZ must therefore have been located within the modern snow petrel foraging range i.e. within ~1200 km from Heimefrontfjella (Fig. 1; Wakefield et al., 2025).

We acknowledge that there are intervals in zone Org-C when the C<sub>14:0</sub> FA record does not align with Cu and cholesterol, which are instead positively correlated with indicators of guano: S and N (Cheng et al., 2016; Tatur et al., 1997; Roberts et al., 2017; Sun et al., 2000; Liu et al., 2005). The negative relationship between C:N and other elements (Cl, P, S) (SI Fig. 7 and 8) also supports a contribution from guano (Berg et al., 2019; Hiller et al., 1988). Although the presence of guano is unlikely to be an issue for interpreting dietary changes, as different biomarkers are involved (e.g. FA C<sub>14:0</sub>, FA C<sub>16:0</sub>, 515 FA C<sub>18:1(n-9)</sub> for diet), it may have contributed to the elevated bulk δ<sup>15</sup>N values in zone Org-C. The δ<sup>15</sup>N values are exceptionally high in zone Org-C (~20%), exceeding those observed in modern Southern Ocean top predators (~12-14 %) (Hückstädt et al., 2012; Valenzuela et al., 2018; Reisinger et al., 2016; Van Den Berg et al., 2021). The increase in  $\delta^{15}$ N is unlikely to reflect higher trophic status (Hodum and Hobson, 2000) or coastal foraging (St John Glew et al., 2021), because the fatty acid distributions suggest high Antarctic krill contributions to the diet, which should introduce lower δ<sup>15</sup>N than fish (Rau et al., 520 1992) and are associated with pelagic foraging (Brault et al., 2018). In zone Org-C, there could be potential for microbial degradation or enhanced guano inputs causing elevated  $\delta^{15}N$ . However, we also note that high  $\delta^{15}N$  are coincident with peak C<sub>14:0</sub> FA fluxes ~6400 cal. yr BP, suggesting foraging could have occurred in pelagic waters with high nitrate utilisation (c.f. (Studer et al., 2018)), consistent with nutrient limitation in highly productive polynyas. The presence of Antarctic krill markers suggests foraging in an open-ocean polynya, such as the intermittent Maud Rise polynya (Fig. 1) (Jena and Pillai, 2020; Turner et al., 2020; Holland, 2001). Feeding at the Maud Rise polynya is possible as snow petrels are able to forage at long ranges >700 km (Honan et al., 2025), although they preferentially feed in broken ice in proximity to their nesting site during chickrearing (Wakefield et al., 2025). Further work is required to identify whether other records with elevated  $\delta^{15}$ N can be identified, or to rule out an impact from guano or degradation on the unusual  $\delta^{15}N$  values in zone Org-C, especially as low %N could indicate degradation. At present, we interpret the data from zone Org-C to reflect foraging in a MIZ situated in pelagic waters

4.2.2 Zone Org-B (5960-4320 cal. vr BP)

Formatted: Font: Bold

Field Code Changed

530 but with the potential for foraging over the continental shelf during intervals when the MIZ was situated closer to the coast.

Between 5960-4320 cal. yr BP, we infer snow petrel foraging which is in a similar or slightly more productive MIZ than in zone Org-C due to elevated contributions from phytol. A mixed diet is inferred from intermediate contributions from C14-0 (FA) and C18-10-9<sub>1</sub>, from Antarctic krill and fish, respectively, with no change in diet compared to zone Org-C based on the fatty acid ratios C16-0/C14-0 and C18-0/C14-0 (Figure 3). This mixed diet continues to indicate feeding both at the continental shelf edge and offshore. The main difference between zones Org-C and Org-B appear to be in the higher %N and sustained inputs of phytol, suggesting a more stable interval of higher productivity (and potentially better preservation) compared to the more variable zone Org-C. High accumulation rates in zone Org-B (Fig. 2) suggest frequent nest occupation during this zone, supported by elevated and sustained accumulation rates for the productivity marker (phytol) (Fig. 3 & 5) and inputs of potential guano-related elements (Fig. 4). Phytol is formed from chlorophyll-a (Rontani and Volkman, 2003) and is brought into snow petrel diet through krill gut contents (Sargent and Falk-Petersen, 1981). As for zone Org-C, foraging in productive waters relatively proximal to the nest site could be explained either by access to foraging in coastal polynyas if the MIZ was situated further offshore, or by a MIZ relatively close to the continent e.g. if winter or spring sea-ice extents are relatively low, enabled in part by ice shelf fronts which were relatively stable during this period (Grieman et al., 2024). The variable but continued presence of Antarctic krill markers implies that there were several intervals where foraging occurred in a MIZ which was situated in pelagic waters between 5960-4320 cal. yr BP.

535

555

560

565

4.2.3 Zone Org-A (4320-1830 cal. yr BP) Our conceptual diagrams (Fig. 5) highlight how we use the geochemical evidence of three zones in the stomach oil deposits to infer changes in of sea lice extent and other oceanographic parameters. In Organic zone C (6700-6200 cal. yr BP) the snow petrel stomach oil accumulation rate was high with geochemical evidence of a diet high in both fish (evidenced by FA C<sub>18.0</sub>) and Antarctic krill (Euphausia superba) (evidenced by FA C<sub>14.0</sub>). Zone C has a short interval of high productivity indicators, which we interpret as a relatively reduced sea lice extent with intermediate sea lice concentration, so that open waters (polynyas) were readily accessible for foraging and is most similar to present day conditions (Fig. 3; Fig 5a). The second period is detailed by organic zone B (6200-4700 cal.

We infer that between 4320-1830 cal. yr BP there was a shift towards a cooler, or neoglacial, phase which is characterised by more extensive sea ice. Our interpretation is based on the lower concentrations and fluxes in most of the organic proxies, aligning with sustained low accumulation rates in zone Org-A (Fig. 2–4). Although we observe no significant changes to diet according to the fatty acid ratios  $C_{160}/C_{14\cdot0}$  and  $C_{18\cdot0}/C_{14\cdot0}$  (Figure 3), the loss of phytol indicates very low primary productivity, and the loss of cholesterol and Cu suggests that contributions from Antarctic krill were also reduced. In zone Org-A we suggest that the low rates of nest occupation and reduction in Antarctic krill and productivity markers indicate limited accessibility to snow petrel prey from the Heimefrontfjella site, which is consistent with the development of a more extensive or more dense sea ice pack in the north-east Weddell Sea which displaced the MIZ further offshore.

Cu) which indicates that foraging was possible beyond the continental shelf edge, but lower fluxes in krill and fish markers (FA  $C_{18:0}$ ) and gradually declining FA  $C_{18:1}$  (mostly krill, but some fish) (Fig. 3) compared to organic zone C suggest

**YF BP)** and features continued contribution of Antarctic krill (Euphausia superba) to the diet ( $C_{14.0}$  (FA), cholesterol,

Formatted: Font: Bold, Italian (Italy)

Formatted: Font: Bold

that this may have been more intermittent. We therefore propose organic zone C as a gradual transition sea ice scenario (Fig. 5b) whereby there was a switch to more coastal (neritic) feeding grounds rich in fish and ice krill, but in slightly less abundance than organic zone C, despite high primary productivity (Fig. 3). We hypothesise that the biogeochemical evidence in organic zone B is consistent with foraging in both open waters within the sea ice (polynyas), which could include at the ice-shelf front, and occasional feeding at the sea-ice edge when foraging range permits. Finally, lower concentrations in most organic proxies and low fluxes of all components to the deposit as accumulation rate falls (Fig. 2-4) is evidenced by a cooler or neoglacial phase organic zone A (4700–2000 cal. yr BP) (Fig. 5c) which is characterised by more extensive sea-ice which limited snow petrel foraging.

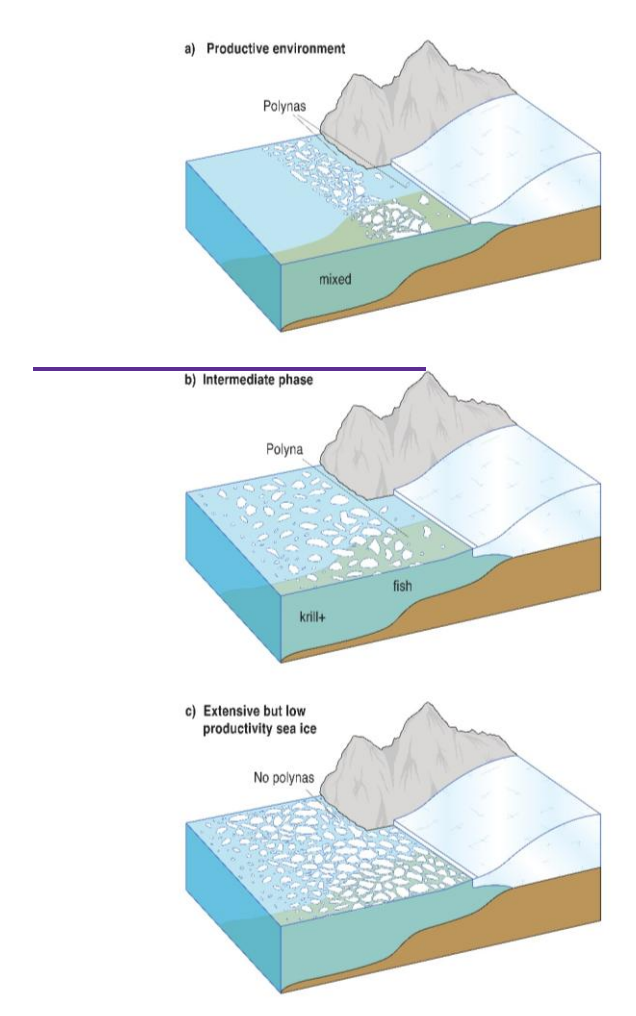


Figure 5: Conceptual diagrams highlighting Antarctic Weddell Sea ice environments interpreted for the three stratigraphic zones in the stomach-oil deposit 3012MUM2 biomarker record. a) Indicates a productive environment similar to current present day ice scenario, with a reduced sea ice extent with intermediate sea ice concentration. For snow petrels this period has more accessible open water with minor sea ice to enable feeding (e.g. zone org-C); b) Indicates an intermediate sea ice configuration inferred from a switch to more coastal feeding grounds. In this scenario feeding will occur in localised polynyas as well as occasional feeding at the sea ice edge where foraging range permits (e.g. zone org-B); c) Indicates a more extensive sea ice and low productivity environment where feeding is blocked by extensive ice (e.g. zone org-A).

#### 4.3 Coherence with other records of Holocene environmental changes in the Weddell Seachange

585

605

610

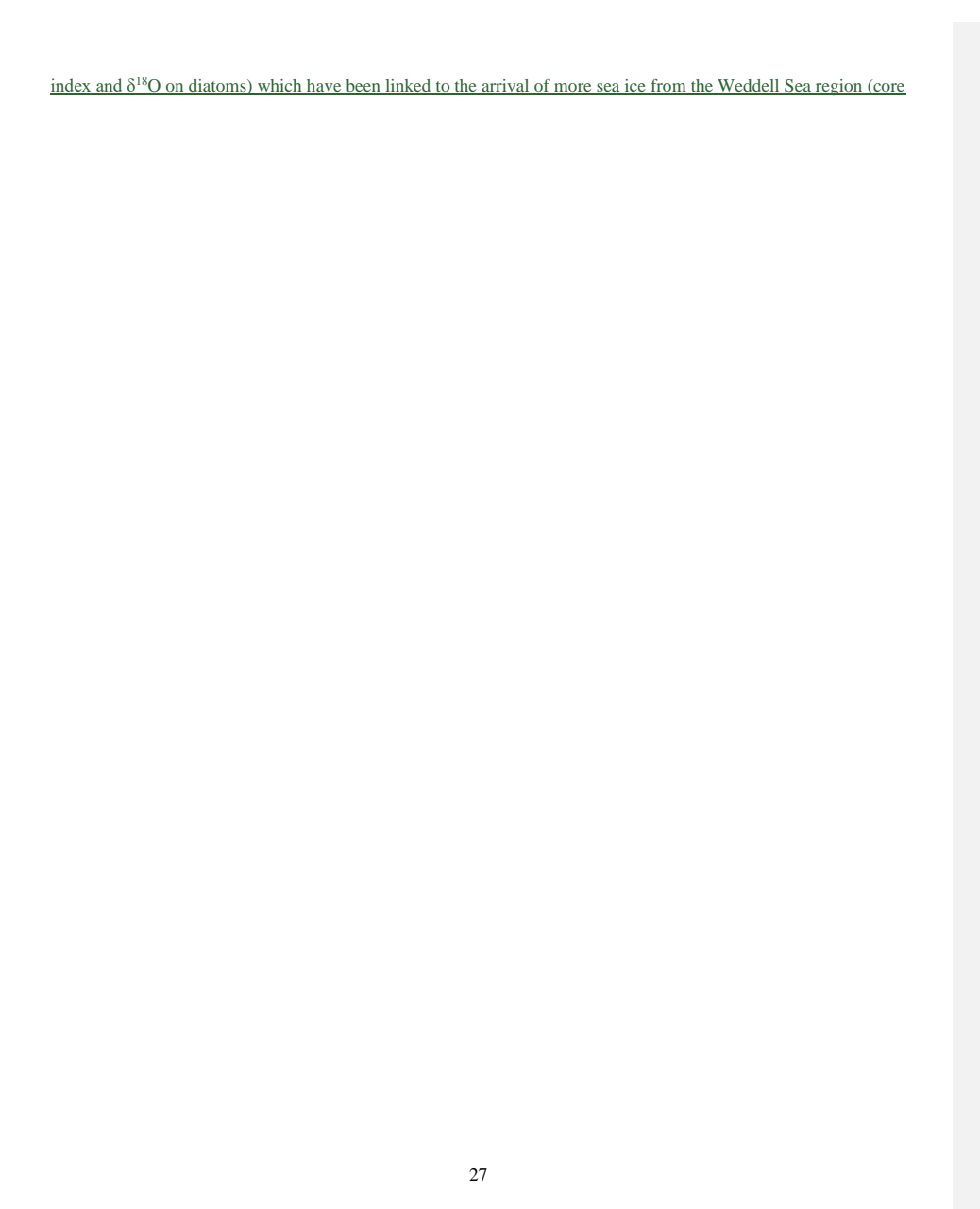
Our records show a clear matchassociations between inference of past sea ice configurations made from our snow petrel stomach oil deposit and proxyregional records of environmental change. For example, there are similarities and differences with records in the wider Weddell Sea region, likely due to both regions being influenced by proximity to the influence of the Weddell Gyre elimate zone and atmospheric processes that determine sea ice configurations. Consistent with Our interpretations of high dietary fatty acid concentrations in our Heimefrontfjella record (organic zone C, 6700–6200productivity and krill between 6390–5960 cal. kyr BP)-( (zone Org-C, Fig. 3 & 6), the HBI (highly branched isoprenoid) sea ice record from the Vega Drift (JPC 38; Fig. 1) features a reduction in sea-ice conditions from around 7.4 ka BP (Barbara et al., 2016) (Fig. 6). A more correspond with a relatively productive and an open-ocean (pelagic) type sea ice configuration was reached by-from 7.2 cal. kyr BP at Herbert Sound and Croft Bay, and suggests in response to a wider regional mid-Holocene warming (e.g. core NBP0502-Site 2) (Totten et al., 2015). In the Firth of Tay (Fig. 1), the mid-Holocene climatic optimum spans 7800–6000 cal. yr BP (core NBP0602A) (Michalchuk et al., 2009) and 7750 and 6000 yr BP (cores NBP0602A-8B and NBP0703-JPC02) (Majewski and Anderson, 2009), and was attributed to seasonally-open marine conditions. Scotia Sea diatom records were are also in phase with our results, with seasonally open water assemblages from 8300 to 2400 yr BP (core SS01) (Bak et al., 2007).

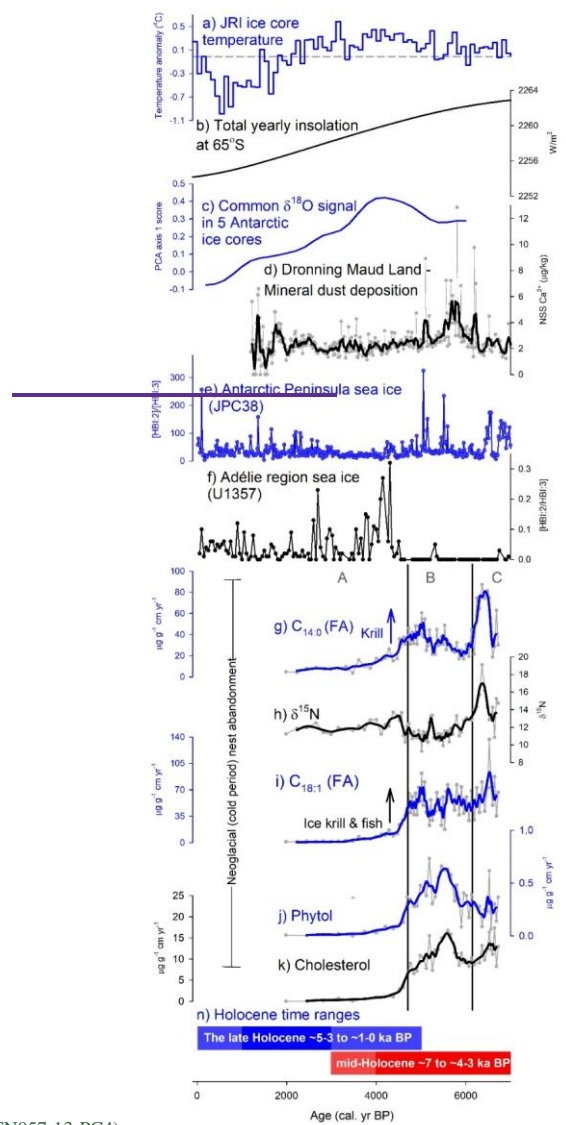
Consistent with gradual transition organic zone B, the biomarker and diatom record at Vega Drift (core JPC38) shows a clear shift to cooler temperatures at ~5 ka BP and associated expansion of the Weddell Gyre (Barbara et al., 2016). At Bransfield Strait (core D1-7) persistent sea ice is observed between 5.8 and 3.8 ka BP (core ANT28/D1-7) (Nie et al., 2022), providing evidence of gradually increasing sea ice extent.

The neoglacial, sea ice expansion and cooling phase in organic zone A is inferred from reduced stomach oil accumulation rates and reduced concentrations of multiple organic markers in the deposit (Fig. 3 & 6). The switch to reduced productivity Our interpretation of zone Org-A having more sea ice corresponds with HBI records at the Vega Drift in JPC38, when interpreted carefully (Fig. 5d) (Barbara et al., 2016). Higher HBI diene levels in our deposit zone Org-A (4320-1830 cal. yr BP) correspond to increased sea ice cover. The fact that HBI:2/HBI:3 ratios vary and are low in zone Org-A are probably due to limitations of the proxy and the issue of normalization, linked with variable pelagic productivity. At Bransfield Strait (core D1-7) persistent sea ice is observed between 5.8 and 3.8 ka BP (core ANT28/D1-7) (Nie et al., 2022).

The neoglacial, sea-ice expansion and cooling phase suggested by zone Org-A is coherent with a sediment record on the Firth of Tay (core NBP0602A-8B and NBP0703-JPC02) which shows cooling from ~3500 yr BP based on foraminifera records (Majewski and Anderson, 2009). At Perseverance Drift, the warm interval persists longer than in our deposit, with high abundance of the foraminifera *Globocassidulina* spp. between 3400 and 1800 yr BP indicating incursions of Weddell Sea Transitional Water and a period of 'freshening' consistent with open-marine or seasonally open marine conditions, followed by its absence from ~1800 yr BP (Kyrmanidou et al., 2018) (cores JKC36 and JPC36):), indicative of cooling.

The boundary between zone Org-B and A (4320 cal. yr BP) aligns with the transition to neoglacial conditions (e.g. (Crosta et al., 2022)). This mid-Holocene neoglacial is consistent with the James Ross Island (JRI) ice core temperature decline (Fig. 5b) (Mulvaney et al., 2012) and decreasing δ<sup>18</sup>O signal in 5 Antarctic ice cores (Hodgson and Bentley, 2013; Masson-Delmotte et al., 2011) (Fig. 5c). We find that the onset of the neoglacial is remarkably in phase with a switch in sea ice biomarkers (both HBI diene and [HBI:2/HBI:3] ratio) indicative of more sea ice in the distant Adélie region in core U1357
 (Ashley et al., 2021) (Fig. 5e). A marked transition is also seen in South Atlantic cores (Hodell et al., 2001) where IRD (as % lithics) increase markedly from ~5 ka BP suggesting cooling waters (together with concomitant changes in diatoms SST





TTN057-13-PC4).

Total yearly insolation (e.g. at 65°S) features an ongoing decline during this period (Fig. 5b) but is unlikely to be the sole driver of the neoglacial (Divine et al., 2010; Renssen et al., 2005).

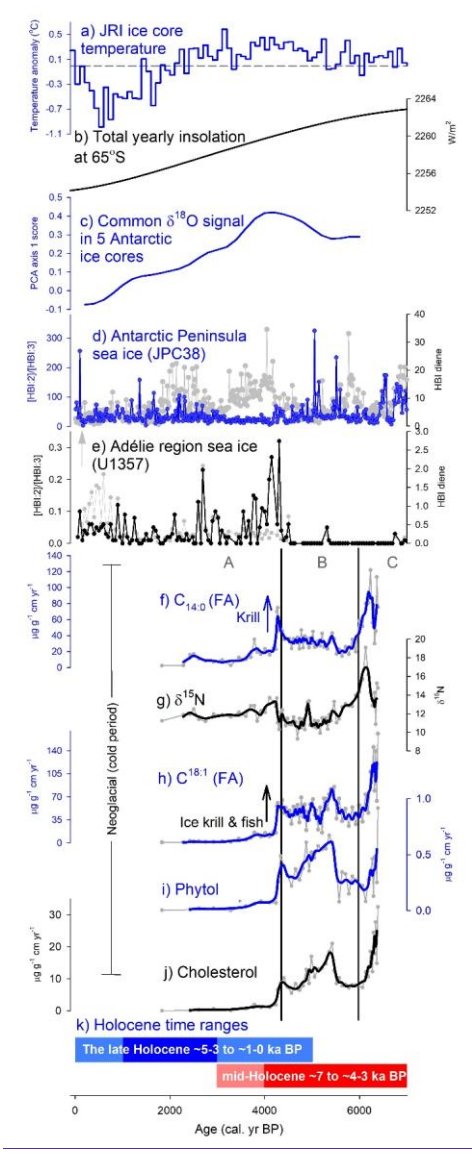


Figure 65: Summary plot comparing the marine and ice-core climate proxies (a-fe) with 3012MUM2 geochemical proxy data (g - kj). (a) James Ross Island (JRI) ice core temperature anomaly relative to 1961-1990 mean based on 100-year averages in Mulvaney et al. (2012); (b) Total yearly insolation at 65°S (Laskar et al., 2004); (c) Common 818O signal in 5 Antarctic ice cores, interpreted by PCA axis 1 scores from Hodgson and Bentley (2013) based on common and residual signals in five Antarctic 818O records; Vostok, Taylor Dome, EPICA Dome C, EPICA Dronning Maud Land and Dome Fuji (Masson-Delmotte et al., 2011); (d) Dronning Maud Land mineral dust deposition from NSS (non-sea salt) Ca<sup>2+</sup>-from the EPICA DML (EDML) ice core (Fischer et al., 2007); (e) Antarctic Peninsula sea ice from the ratio of highly-branched isoprenoid (HBI) diene to triene and HBI diene individually (core JPC38) (Barbara et al., 2016); (fe) Adélie region sea ice from the ratio of HBI diene to triene and HBI diene individually (core U1257) (Ashley et al., 2021); (gf) C<sub>140</sub> (FA) flux as a krill maker; (hg) nitrogen stable isotopes (8<sup>15</sup>N); (hl) C<sub>181(10-91</sub> (FA) as an ice krill and fish marker; (hg) phytol flux as a productivity marker; (kg) cholesterol flux; and (nk) Holocene time ranges for palaeoclimate periods from Crosta et al. (2022). Smooth lines are calculated from appropriate moving averages. Cluster boundaries (vertical black lines) are based in organie-zones Org-A-C in Fig.3.

#### 4.4 Reconstructing ocean productivity using snow-petrel stomach oil markers

650

660

For the first time we find significant utility in stomach oil phytol and cholesterol as markers of ocean productivity and diet (Fig. 3 & 6). Phytol is formed from chlorophyll a (Rontani and Volkman, 2003) and is brought into snow petrel diet through krill gut contents (Sargent and Falk-Petersen, 1981). Cholesterol is ubiquitous in living matter but is especially high in krill (Ju and Harvey, 2004), and lower in fish. In the stomach oil record the phytol record is highest in the gradual transition ice organic zone B, indicating access to phytoplankton-rich foraging grounds (greater than in the warmest period e.g. organic zone C) both in the open ocean type configuration and within coastal polynyas scenarios (Fig. 5) close to ice shelves which were in a retreating phase prior to/around this time (Grieman et al., 2024). In organic zone B high nitrogen-containing pigments may have contributed to elevated nitrogen levels. It is also likely that during this period of high accumulation rate (organic zone B) there may also have been enhanced preservation of N containing compounds.

Importantly, cholesterol is highest in zone organic C, a period which we interpret from fatty acid signatures to have had highest dietary abundances of both fish and krill. Phytol and cholesterol likely reflect evidence of high productivity krill-rich polynyas (coastal or open ocean types). Here we interpret high productivity (evidenced by high phytol) as an expression of the ice shelf front polynya moving south through the foraging range (see zone organic C). The retreating ice edge with associated coastal polynyas could also potentially lead to more frequent occupation of the nest site and concomitant high stomach oil accumulation.

#### 655 4.5 Isotopic shifts coherent with mid-Holocene warming, increased productivity and potential opening of the Maud Rise polynya

Maud Rise polynya which forms intermittently above Maud Rise plateau (Fig. 1) Jena and Pillai, 2020; Turner et al., 2020; Holland, 2001). High contributions of Antarctic krill in organic zone C (e.g. peak C<sub>1+0</sub> FA fluxes -6400 cal. FPP) are coincident with a high δ<sup>15</sup>N (--20 ‰) (Fig. 3). The δ<sup>15</sup>N values are exceptionally high, exceeding those observed in modern southern ocean top predators (-12 14 ‰) (Hückstädt et al., 2012; Valenzuela et al., 2018; Reisinger et al., 2016; Van Den Berg et al., 2021). The increase in δ<sup>15</sup>N is unlikely to reflect high trophic status, because the high Antarctic krill contributions would be expected to introduce lower δ<sup>15</sup>N than fish (Rau et al., 1992). Nor can a shift towards coastal foraging, where δ<sup>15</sup>N

The combination of elevated  $\delta^{15}$ N and fatty acid concentrations in the early part of the record may reflect an opening of the

Field Code Changed

Formatted: Font: Bold, Italian (Italy)

values are high (St John Glew et al., 2021), offer an explanation, because the fatty acid markers clearly indicate a mixed diet requiring contributions from both fish and krill (Fig. 3). Instead, we suggest that a baseline shift in  $\delta^{45}$ N occurred, whereby enhanced nutrient delivery was facilitated by upwelling, potentially of circumpolar deep water (CDW). In turn<sub>7</sub> elevated productivity would have been stimulated, evidenced by the high phytol fluxes at this time.

665

670

680

685

690

695

We argue that the high krill consumption is probably linked to the enhanced opening of the large open-ocean Maud Rise polynya, which we posit may give space for early productivity, due to more ice free environments when solar radiation starts to increase in the austral spring (e.g. (Goosse et al., 2021; Jena et al., 2019; Von Berg et al., 2020)). Changes in wind activity may also play a role in Maud Rise polynya formation, much as it does today (Zhou et al., 2022; Francis et al., 2019). Opening of polynyas typically lead to higher productivity and the potential for higher krill (Kang et al., 2020; La et al., 2015). A palaeoreconstruction over the past ~700 years from the sub-Antarctic Marion Island highlight how during cooler periods (e.g. Little Ice Age), winds weakened moving towards the equator, but during warm periods they increased and transitioned towards the pole (Perren et al., 2020). Therefore, it seems feasible that latitudinal shifts in the core wind belt over the Holocene could contribute to changes in the Maud Rise polynya, helping to explain shifts between organic zones (Fig. 3 & 5).

# 4.6 Synchrony between the north west Weddell Sea sea ice stomach-oil record and Southern Hemisphere palaeoclimate records

There are wider similarities between our Weddell Sea sea ice record and proxy records from the continental ice sheet, from Southern Ocean sediments, and in coastal sediments the opposite side of Antarctica, off Adélie Land, pointing to broader earth-system changes over the Holocene (e.g., insolation forcing, oceanographic and ice sheet changes) (Fig. 6).

Broader changes in stomach oil deposit 3012MUM2, which point to a more productive organic zone C and part of organic zone B compared with a less productive organic zone Λ identify the widely recognised hypsithermal to neoglacial transition [e.g. (Crosta et al., 2022)]. Changes between the two periods are congruous with an early and productive mid-Holocene warming (also referred to as the Hypsithermal; (Bentley et al., 2009). Climate warming was broadly consistent with ice loss in parts of the Antarctic Peninsula (Johnson et al., 2019; Totten et al., 2015; Michalchuk et al., 2009; Majewski and Anderson, 2009) and completion of the retreat of Filchner and Ronne Ice Shelf (Hillenbrand et al., 2014). The general mid-Holocene warming to neoglacial transition is also consistent with James Ross Island (JRI) ice core temperature in the northwestern Weddell Sea (Mulvaney et al., 2012) which begins to decline from its highest point ~3100 yr BP (Fig. 6). It is further consistent with the broader decreasing δ<sup>18</sup>O signal in 5 Antarctic ice cores, interpreted by PCA axis 1 scores based on common and residual signals in δ<sup>18</sup>O records (Hodgson and Bentley, 2013; Masson-Delmotte et al., 2011) (Fig. 6). Remarkably, high non sea salt deposition (Ca<sup>2+</sup>) from ice cores taken in Dronning Maud Land reflecting wind blown dust—predominantly from Patagonia (Fischer et al., 2007) is broadly in line with the period of high phytol (indicating high primary productivity) (Fig. 6). An exact causal mechanism between the two records is uncertain as dust is unlikely to be sufficient to stimulate algae at the oceanographic scale at Holocene timescales, even though it can at glacial timescales (Martínez-Garcia et al., 2009; Martínez-Garcia et al., 2011). However even slight changes in wind patterns and intensity can also affect sea ice

cover which we purport to be a more likely potential driver typically linked to stratification and iron imitation [e.g. (Sigman et al., 2004; Martínez Garcia et al., 2009)] and enable both deposition of dust on Antarctica while also influencing decadal-scale sea ice cover-

700

710

715

720

Sea ice cover also shows wider southern hemispheric patterns. Off the Antarctic Peninsula (JPC38 — South Eastern tip) there was a slightly higher ratio of sea ice dwelling diatoms (HBI diene) compared with pelagic diatoms (HBI triene) in organic zones B and C of deposit 3012MUM2, compared with the more 'neoglacial' cooler organic zone A (Barbara et al., 2016) (Fig. 6). The HBI ratio is complex as environments with high HBI diene (intermediate presence of sea ice (Belt et al., 2016)) are likely to be ideal environments for snow petrel feeding given their close affinity to sea ice (Delord et al., 2016; Ainley and Jacobs, 1981; Ainley et al., 2017), providing confidence that the neighbouring Weddell Sea was likely to have been a good environment for feeding, consistent with the productive and rich deposit at this time. However, remarkably the transition around ~4700 cal. yr BP to cooler, neoglacial conditions in deposit 3012MUM2 is contemporaneous with a distinct switch to more sea ice in the distant Adélie region at the opposite side of Antarctica, inferred by HBI ratios in core U1357 (Ashley et al., 2021) (Fig. 6F). Ashley et al. (2021) suggest that although the mechanistic driver is not fully resolved, a potential explanation could be the retreat of grounded ice, development of large ice shelf cavities and subsequent altering of AABW and AASW (Antarctic Surface Water). The wider timing of this key transition evidenced in 3012MUM2 ~4700 cal. yr BP could point to a similar mechanism in the Weddell Sea, linked to "ice pump" enhancement of sub-ice shelf-circulation, facilitating the non-linear transition observed (Ashley et al., 2021).

Remarkably the key shift (evidenced between organic zones A & B, ~4700) in the stomach oil deposit is also in phase with a marked transition-seen in South Atlantic cores (Hodell et al., 2001) where IRD (as % lithics) increase markedly from -5 ka BP suggesting cooling waters (together with concomitant changes in diatoms SST index and 8<sup>48</sup>O on diatoms) which have been linked to the arrival of more sea ice from the Weddell Sea region (core TTN057-13-PC4). Hodell et al. (2001) highlight the wider similarities with non linear responses in gradual changes in the Northern Hemisphere, coinciding with rapid changes in middle Holocene climate evidenced from Taylor Dome ice core (Steig et al., 1998). This sediment core record highlights the switch between the mid Holocene warming and the beginning of neoglacial in the mid Holocene (Hodell et al., 2001). Divine et al. (2010) highlight similar transitions in more cores (also TN057-17-PC1 & TN057-13-PC4) in the Southern Ocean pointing to a clear neoglacial after ~4000 yr BP associated with strengthening of the westerlies and cooling in the inland ice sheet. Hodell et al. (2001) suggest a wider mechanism—although as yet unconfirmed—could be broadly related to insolation changes generating complex feedback at different latitudes of the Southern Ocean and Northern Hemisphere. In terms of insolation, although the Southern Ocean broadly saw an increase in summer insolation from the start of the record, total yearly insolation (e.g. at 65°S) features a decline, providing evidence of an overarching mechanism which may contribute to the mid-Holocene warming to neoglacial transition (Fig. 6). However, modelling suggests that insolation is unlikely to be the sole driver of the transition (Divine et al., 2010; Renssen et al., 2005); variations in sea ice extent in the Southern Ocean are suggested to be a more important driver (Knorr and Lohmann, 2003). The convincing detailed responses in productivity.

(30) accumulation, and dietary source markers in deposit 3012MUM2 [e.g. accumulation rates of cholesterol, phytol and fatty acids (Fig. 6)] highlight the role of regional oceanographic and sea ice dominated forcings.

#### 5 Conclusions

Analyses of accumulation rates and a range of biomarkers in a snow petrel stomach-oil deposit from the Heimefrontfjella Range have been used to infer sea ice and climate in the northeastern Weddell Sea over the Holocene. The record broadly 735 follows a three-zone Holocene climate evolution consistent with changes recorded in the northwestern Weddell Sea and wider regional patterns seen in Antarctica and the Southern Ocean (Crosta et al., 2022). In the first stage between 6700-6200 cal. yr BPconditions in the foraging area in the northeastern Weddell Sea over the Holocene. The record has three significant zones. In the first zone between 6390-5960 cal. yr BP, high stomach oil accumulation rates and high concentrations of both fish and krill fatty acids suggest easy access to productive foraging grounds. This is consistent with low sea ice cover and extensive 740 polynyas associated with warmer temperatures and regional ice shelf retreat. In the second stage, between 6200-4700 cal. yr BP reductions in accumulation rates of both Antarctic krill fatty acids (e.g. C<sub>14:0</sub>) and fatty acids mainly from fish (e.g. C<sub>18:0</sub>) are used to infer a gradual transition to a more extensive sea ice configuration restricting access to pelagic foraging grounds. This is consistent with a switch towards both at the continental shelf in the MIZ and offshore. In the second zone, between 5960-4320 cal. yr BP productivity remained high but there was evidence of a more mixed diet suggesting foraging in coastal 745 polynyas both at the ice-continental shelf front.edge and in open water, with high productivity due to summer sea ice retreat reaching the shelf edge more frequently. In the third stage, between 46004320 and 20001830 cal. yr BP low stomach oil accumulation rates and reductions in fatty acid and productivity markers indicate that increased sea ice extent restricted access to foraging grounds and by ~6700 cal. yr BP resulted in abandonment of the nest site. This is conditions consistent with the transition to-cooler neoglacial conditions seen in a range of records from the northwestern Weddell Sea (Barbara et al., 2016; Nie et al., 2022), from ice records on the Antarctic continent (Hodgson and Bentley, 2013), and changes elsewhere in the wider 750 Antarctic region including Adélie Land (Ashley et al., 2021) and the South Atlantic (Hodell et al., 2001; Divine et al., 2010). This study has also shown, for the first time, the utility of phytol and cholesterol for tracking past snow petrel diet and thus interpretation of environmental conditions- in their foraging areas.

Formatted: Highlight

Data availability

55 All data presented within this manuscript has been submitted to data repository PANGAEA (PDI-40423)

#### Author contributions

ELM obtained main funding. MAS, DRG, NT, CL, AG & ELM carried out the laboratory work and data analysis. MJB & DAH collected samples from Antarctica. MAS prepared the initial paper and revised the manuscript during the review process, discussing initial primary interpretations with ELM, MJB & DAH.

# 760 Competing interests

Some authors are members of the editorial board of the journal Climate of the Past. The authors also have no other competing interests to declare.

#### Acknowledgements

We thank the BAS field operations staff and pilots who supported the work along with Andy Hein and Al Davies who helped with field sampling. We thank Kerry A. Strong, Martin D. West and Amanda Hayton for laboratory assistance. We also thank Helen Mackay for advice and assistance regarding the interpretation of sterols and stanols. We thank Ewan Wakefield for insights on snow petrel feeding ranges and seasonality, plus James Grecian for discussion of Southern Ocean/Weddell Sea species distribution references. We also thank Chris Orton for drafting Figure 5 We also thank Richard Staff for assistance with OxCal. We thank an anonymous reviewer and Xavier Crosta for helpful comments on the manuscript during the review process.

# Financial support

This research was supported by the European Research Council H2020 (ANTSIE (grant no. 864637)) and the Leverhulme Trust (Philip Leverhulme Research Leadership Award, RL-2019-023). Deposit 3012MUM2 was collected as part of a NERC-funded award to MB and DH on past ice sheet and environmental change in Coats Land (Reference: NE/K003674/1).

#### 775 References

Ainley, D., Woehler, E. J., and Lescroël, A. Birds and Antarctic sea ice, in: Sea Ice 570-582 doi: 10.1002/9781118778371, 2017.

Ainley, D. G. and Jacobs, S. S. Sea bird affinities for ocean and ice boundaries in the Antarctic *Deep Sea Research Part A. Oceanographic Research Papers* 28 1173–1185, 1981.

Ai, X. E., Studer, A. S., Sigman, D. M., Martínez-García, A., Fripiat, F., Thöle, L. M., Michel, E., Gottschalk, J., Arnold, L., Moretti, S., Schmitt, M., Oleynik, S., Jaccard, S. L., and Haug, G. H.: Southern Ocean upwelling, Earth's obliquity, and glacial-interglacial atmospheric CO<sub>2</sub> change, Science, 370, 1348-1352, 10.1126/science.abd2115, 2020.

Ainley, D. G., O'Connor, E. F., and Boekelheide, R. J., The Marine Ecology of Birds in the Ross Sea, Antarctica, Ornithological Monographs, iii-97, 10.2307/40166773, 1984.

Formatted: German (Germany)

Formatted: German (Germany)

Formatted: German (Germany)

Formatted: Font: Not Italic, German (Germany)

Formatted: German (Germany)

Formatted: German (Germany)

785	Ainley, D. G., Jacobs, S. S., Ribic, C. A., and Gaffney, In. Seabird distribution and oceanic features of the Amundsen and	-	Formatted	
	southern Bellingshausen seas, Antarctic Science, 10, 111-123, 10.1017/S0954102098000169, 1998.			
	Ainley, D. G., Hobson, K. A., Crosta, X., Rau, G. H., Wassenaar, L. I., and Augustinus, P. C., Holocene variation in the	-1	Formatted	(
	Antarctic coastal food web: linking &D and & 13C in snow petrel diet and marine sediments. Mar. Ecol. Prog. Ser. 306, Marine	// `		`
	Ecology Progress Series, 306, 31-40, 2006.			
790	Arrigo, K. R., Lubin, D., van Dijken, G. L., Holm-Hansen, O., and Morrow, E.: Impact of a deep ozone hole on Southern			
	Ocean primary production, Journal of Geophysical Research: Oceans, 108, https://doi.org/10.1029/2001JC001226, 2003.			
	Ashley, K. E., McKay, R., Etourneau, J., Jimenez-Espejo, F. J., Condron, A., Albot, A., Crosta, X., Riesselman, C., Seki, O.,	-	Formatted	
	Massé, G., Golledge, N. R., Gasson, E., Lowry, D. P., Barrand, N. E., Johnson, K., Bertler, N., Escutia, C., Dunbar, R., and			(
	Bendle, J. A., Mid-Holocene Antarctic sea-ice increase driven by marine ice sheet retreat Clim. Past, 17, 1-19, 10.5194/cp-	//		
795	17-1-2021, 2021.			
	Bak, YS., Yoo, KC., Yoon, H. I., Lee, JD., and Yun, H., Diatom evidence for Holocene paleoclimatic change in the South	_	Formatted	(
	Scotia Sea, West Antarctica, Geosciences Journal, 11, 11-22, 10.1007/BF02910377, 2007.			(
	Barbara, L., Crosta, X., Massé, G., and Ther, O.: Deglacial environments in eastern Prydz Bay, East Antarctica Quaternary		Formatted	(
	Science Reviews, 29, 2731-2740, 2010.https://doi.org/10.1016/j.quascirev.2010.06.027, 2010.		F	(
800	Barbara, L., Crosta, X., Schmidt, S., and Massé, G. Diatoms and biomarkers evidence for major changes in sea ice conditions		Formatted: German (Germany)	
	prior the instrumental period in Antarctic Peninsula, Quaternary Science Reviews, 79, 99-110,		Formatted	
	https://doi.org/10.1016/j.quascirev.2013.07.021,2013.		Formatted: German (Germany)	
	Barbara, L., Crosta, X., Leventer, A., Schmidt, S., Etourneau, J., Domack, E., and Massé, G., Environmental responses of the		Formatted	
	Northeast Antarctic Peninsula to the Holocene climate variability, Paleoceanography, 31, 131-147,		romatteu	
805	https://doi.org/10.1002/2015PA002785, 2016.		Formatted: German (Germany)	
	Belt, S. T., Smik, L., Brown, T. A., Kim, J. H., Rowland, S. J., Allen, C. S., Gal, J. K., Shin, K. H., Lee, J. I., and Taylor, K.		. "	
	W. Source identification and distribution reveals the potential of the geochemical Antarctic sea ice proxy IPSO <sub>25</sub> Nature			
	Communications 7 1 10, 2016.			
	Bennett, K. D.: Determination of the number of zones in a biostratigraphical sequence, New Phytologist, 132, 155-170, 4996.		Formatted: Font: Not Italic	
810	Bentley, M. J., Hodgson, D. A., Smith, J. A., Cofaigh, C. Ó., Domack, E. W., Larter, R. D., Roberts, S. J., Brachfeld, S.,	_ (		
	Leventer, A., Hjort, C., Hillenbrand, C. D., and Evans, J. Mechanisms of Holocene palaeoenvironmental change in the			
	Antarctic Peninsula region The Holocene 19.51-69, 2009https://doi.org/10.1111/j.1469-8137.1996.tb04521.x, 1996.		Formatted: German (Germany)	
	Bentley, M. J., Ó Cofaigh, C., Anderson, J. B., Conway, H., Davies, B., Graham, A. G. C., Hillenbrand, CD., Hodgson, D.	- (		
	A., Jamieson, S. S. R., Larter, R. D., Mackintosh, A., Smith, J. A., Verleyen, E., Ackert, R. P., Bart, P. J., Berg, S., Brunstein,			
815	D., Canals, M., Colhoun, E. A., Crosta, X., Dickens, W. A., Domack, E., Dowdeswell, J. A., Dunbar, R., Ehrmann, W., Evans,			
	J., Favier, V., Fink, D., Fogwill, C. J., Glasser, N. F., Gohl, K., Golledge, N. R., Goodwin, I., Gore, D. B., Greenwood, S. L.,			
	Hall, B. L., Hall, K., Hedding, D. W., Hein, A. S., Hocking, E. P., Jakobsson, M., Johnson, J. S., Jomelli, V., Jones, R. S.,			
	Klages, J. P., Kristoffersen, Y., Kuhn, G., Leventer, A., Licht, K., Lilly, K., Lindow, J., Livingstone, S. J., Massé, G., McGlone,			
	M. S., McKay, R. M., Melles, M., Miura, H., Mulvaney, R., Nel, W., Nitsche, F. O., O'Brien, P. E., Post, A. L., Roberts, S. J.,			
820	Saunders, K. M., Selkirk, P. M., Simms, A. R., Spiegel, C., Stolldorf, T. D., Sugden, D. E., van der Putten, N., van Ommen,			
	T., Verfaillie, D., Vyverman, W., Wagner, B., White, D. A., Witus, A. E., and Zwartz, D., A community-based geological	$\rightarrow$	Formatted	(
	reconstruction of Antarctic Ice Sheet deglaciation since the Last Glacial Maximum, Quaternary Science Reviews, 100, 1-9,	/ `		(
	https://doi.org/10.1016/j.quascirev.2014.06.025_2014.		Formatted: German (Germany)	
	Berg, S., Melles, M., Hermichen, WD., McClymont, E. L., Bentley, M. J., Hodgson, D. A., and Kuhn, G., Evaluation of		Formatted	
825	Mumiyo Deposits From East Antarctica as Archives for the Late Quaternary Environmental and Climatic History		Torridated	(
	Geochemistry, Geophysics, Geosystems 20, 260-276, https://doi.org/10.1029/2018GC008054, 2019.	_	Formatted: German (Germany)	
	Berg, S., Emmerson, L., Heim, C., Buchta, E., Fromm, T., Glaser, B., Hermichen, WD., Rethemeyer, J., Southwell, C., Wand,	`		
	U., Zech, M., and Melles, M., Reconstructing the Paleo-Ecological Diet of Snow Petrels (Pagodroma nivea) From Modern	1	Formatted	(
	Samples and Fossil Deposits: Implications for Southern Ocean Paleoenvironmental Reconstructions, Journal of Geophysical	//`		(
830	Research: Biogeosciences 128 e2023JG007454, https://doi.org/10.1029/2023JG007454, 2023.	_	Formatted: German (Germany)	
	Bianchi, C. and Gersonde, R.: Climate evolution at the last deglaciation: the role of the Southern Ocean, Earth and Planetary			
	Science Letters, 228, 407-424, https://doi.org/10.1016/j.epsl.2004.10.003, 2004.			

	Björck, S., Hjort, C., Ingólfsson, O., and Skog, G; Radiocarbon dates from the Antarctic Peninsula – problems and potential,	_	Formatted	(
	in: Radiocarbon Dating: Recent Applications and Future Potential, edited by: Lowe, J. J., Quaternary Research Association	//		
835	Cambridge, 55-65, 1991a.			
	Björck, S. H., C. Ingófsson, O. Skog, G.: Radiocarbon dates from the Antarctic Peninsula problems and potential, Radiocarbon			
	Dating: Recent Applications and Future Potential. Quat. Proc., 1, Cambridge, 55-56, 1991b.		Formatted: German (Germany)	
	Blaauw, M. and Christen, J. A. Flexible paleoclimate age-depth models using an autoregressive gamma process Bayesian Anal.			
	<del>6 457 474, 2011.</del>			
840	Blaauw, M., Christen, J. A., Lopez, M. A. A., Vazquez, J. E., Belding, T., Theiler, J., Gough, B., Karney, C., Rcpp, L., and			
	Blaauw, M. M. Package 'rbacon' 2023.			
	Bokhorst, S., Huiskes, A., Convey, P., and Aerts, R.: External nutrient inputs into terrestrial ecosystems of the Falkland Islands			
	and the Maritime Antarctic region, Polar Biology, 30, 1315-1321, 10.1007/s00300-007-0292-0, 2007.			
	Brandon, M. A., Cottier, F. R., and Nilsen, F.: Sea Ice and Oceanography, in: Sea Ice 2nd Edition ed., edited by: Thomas,	_	Formatted	
845	D. N., and Dieckmann, G., S., Wiley-Blackwell, Chichester, United Kingdom, 79-111, 2010.			,
	Brault, E. K., Koch, P. L., McMahon, K. W., Broach, K. H., Rosenfield, A. P., Sauthoff, W., Loeb, V. J., Arrigo, K. R., and			
	Smith Wo, Jr.: Carbon and nitrogen zooplankton isoscapes in West Antarctica reflect oceanographic transitions, Marine			
	Ecology Progress Series, 593, 29-45, 2018.			
	Bridges, C.: Structure and function of krill (Euphasia superba) hemocyanin-adaption to life at low temperature, Structure and	_	Formatted	
850	function of invertebrate respiratory proteins Life Chemistry Reports 1,353-356, 1983.			
	Bronk Ramsey, C.: Bayesian Analysis of Radiocarbon Dates, Radiocarbon, 51, 337-360, 10.1017/S0033822200033865, 2009.			
	Castro, M. F., Neves, J. C. L., Francelino, M. R., Schaefer, C. E. G. R., and Oliveira, T. S. Seabirds enrich Antarctic soil with	-	Formatted	
	trace metals in organic fractions Science of The Total Environment, 785, 147271,			
	<del>2021.</del> https://doi.org/10.1016/j.scitotenv.2021.147271, 2021		Formatted: German (Germany)	
855	Chen, T., Robinson, L. F., Li, T., Burke, A., Zhang, X., Stewart, J. A., White, N. J., and Knowles, T. D. J.: Radiocarbon			
	evidence for the stability of polar ocean overturning during the Holocene, Nature Geoscience, 16, 631-636, 10.1038/s41561-			
	<u>023-01214-2, 2023.</u>			
	Cheng, W., Sun, L., Kimpe, L. E., Mallory, M. L., Smol, J. P., Gallant, L. R., Li, J., and Blais, J. M., Sterols and Stanols	1	Formatted	
0.40	Preserved in Pond Sediments Track Seabird Biovectors in a High Arctic Environment, Environmental Science & Technology	//		
860	50, 9351-9360, 10.1021/acs.est.6b02767, 2016.			
	Clarke, A.: Lipid Content and Composition of Antarctic Krill, Euphausia Superba Dana, Journal of Crustacean Biology, 4,			
	285-294, 10.1163/1937240x84x00660, 1984.			
	Collins, M., Knutti, R., Arblaster, J., Dufresne, JL., Fichefet, T., Friedlingstein, P., Gao, X., Gutowski, W. J., Johns, T., and	1	Formatted	(.
0.05	Krinner, G., Long-term climate change: projections, commitments and irreversibility, in: Climate Change 2013-The Physical	_/_		
865	Science Basis: Contribution of Working Group I to the Fifth Assessment Report of the Intergovernmental Panel on Climate Change, Cambridge University Press, 1029-1136, 2013.			
	Comiso, J. C. and Gordon, A. L., Recurring polynyas over the Cosmonaut Sea and the Maud Rise, Journal of Geophysical			
	Research: Oceans, 92, 2819-2833, https://doi.org/10.1029/JC092iC03p02819, 1987.	$\overline{}$	Formatted	( .
	Connan, M., Mayzaud, P., Trouvé, C., Barbraud, C., and Cherel, Y.: Interannual dietary changes and demographic		Formatted: German (Germany)	
870	consequences in breeding blue petrels from Kerguelen Islands, Marine Ecology Progress Series, 373, 123-135, 2008.			
0/0	Cripps, G. C., Watkins, J. L., Hill, H. J., and Atkinson, A., Fatty acid content of Antarctic krill Euphausia superba at South		F	
	Georgia related to regional populations and variations in diet, Mar. Ecol. Prog. Ser., 181, 177-188, 1999.	/	Formatted	
	Crosta, X., Denis, D., and Ther, O.: Sea ice seasonality during the Holocene, Adélie Land, East Antarctica, Marine			
	Micropaleontology, 66, 222-232, https://doi.org/10.1016/j.marmicro.2007.10.001, 2008.			
875	Crosta, X., Etourneau, J., Orme, L. C., Dalaiden, Q., Campagne, P., Swingedouw, D., Goosse, H., Massé, G., Miettinen, A.,			
075	McKay, R. M., Dunbar, R. B., Escutia, C., and Ikehara, M.: Multi-decadal trends in Antarctic sea-ice extent driven by ENSO—			
	SAM over the last 2,000 years, Nature Geoscience, 14, 156-160, 10.1038/s41561-021-00697-1, 2021.			
	Crosta, X., Kohfeld, K. E., Bostock, H. C., Chadwick, M., Du Vivier, A., Esper, O., Etourneau, J., Jones, J., Leventer, A.,		Formatted	
	Müller, J., Rhodes, R. H., Allen, C. S., Ghadi, P., Lamping, N., Lange, C. B., Lawler, K. A., Lund, D., Marzocchi, A., Meissner,		rormatted	
880	K. J., Menviel, L., Nair, A., Patterson, M., Pike, J., Prebble, J. G., Riesselman, C., Sadatzki, H., Sime, L. C., Shukla, S. K.,			
000	Thöle, L., Vorrath, M. E., Xiao, W., and Yang, J., Antarctic sea ice over the past 130 000 years – Part 1: a review of what	//		
	proxy records tell us_Clim. Past_18_1729-1756, 10.5194/cp-18-1729-2022, 2022.	/		
	K - A			

	Delord, K., Pinet, P., Pinaud, D., Barbraud, C., De Grissac, S., Lewden, A., Cherel, Y., and Weimerskirch, H., Species-specific	-/	Formatted	
	foraging strategies and segregation mechanisms of sympatric Antarctic fulmarine petrels throughout the annual cycle "Ibis.	//		
885	158, 569-586, https://doi.org/10.1111/ibi.12365, 2016.		Formatted: German (Germany)	
	Denis, D., Crosta, X., Barbara, L., Massé, G., Renssen, H., Ther, O., and Giraudeau, J., Sea ice and wind variability during	-	Formatted	
	the Holocene in East Antarctica: insight on middle-high latitude coupling Quaternary Science Reviews, 29, 3709-3719,			
	https://doi.org/10.1016/j.quascirev.2010.08.007, 2010.  Divine, D. V., Koç, N., Isaksson, E., Nielsen, S., Crosta, X., and Godtliebsen, F., Holocene Antarctic climate variability from		Formatted: German (Germany)	
890	ice and marine sediment cores: Insights on ocean–atmosphere interaction, Quaternary Science Reviews, 29, 303-312,		Formatted	
090	https://doi.org/10.1016/j.quascirev.2009.11.012, 2010.	_	Formatted: German (Germany)	
	Duda, M. P., Hargan, K. E., Michelutti, N., Blais, J. M., Grooms, C., Gilchrist, H. G., Mallory, M. L., Robertson, G. J., and		Formatted: Germany)	
	Smol, J. P.: Reconstructing Long-Term Changes in Avian Populations Using Lake Sediments: Opening a Window Onto the			
	Past, Frontiers in Ecology and Evolution, Volume 9 - 2021, 10.3389/fevo.2021.698175, 2021.			
895	Eayrs, C., Li, X., Raphael, M. N., and Holland, D. M., Rapid decline in Antarctic sea ice in recent years hints at future change.	_	Formatted	
	Nature Geoscience, 14, 460-464, 10.1038/s41561-021-00768-3, 2021.			()
	Etourneau, J., Collins, L. G., Willmott, V., Kim, J. H., Barbara, L., Leventer, A., Schouten, S., Sinninghe Damsté, J. S.,			
	Bianchini, A., Klein, V., Crosta, X., and Massé, G., Holocene climate variations in the western Antarctic Peninsula: evidence	-	Formatted	
	for sea ice extent predominantly controlled by changes in insolation and ENSO variability, Clim. Past, 9, 1431-1446.	// `		
900	10.5194/cp-9-1431-2013 <b>, 2013</b> .	′ ,		
	Ferrari, R., Jansen, M. F., Adkins, J. F., Burke, A., Stewart, A. L., and Thompson, A. F., Antarctic sea ice control on ocean	-/	Formatted	()
	circulation in present and glacial climates, Proceedings of the National Academy of Sciences, 111, 8753-8758,	/		
	doi:10.1073/pnas.1323922111, 2014.			
005	Fetterer, F., Knowles, K., Meier, W., Savoie, M., and Windnagel, A.: Updated daily. Sea Ice Index, Version 3, Boulder,			
905	Colorado USA. NSIDC: National Snow and Ice Data Center, 10.7265/N5K072F8, 2017.			
	Fischer, H., Fundel, F., Ruth, U., Twarloh, B., Wegner, A., Udisti, R., Becagli, S., Castellano, E., Morganti, A., Severi, M.,			
	Wolff, E., Littot, G., Röthlisberger, R., Mulvaney, R., Hutterli, M. A., Kaufmann, P., Federer, U., Lambert, F., Bigler, M., Hansson, M., Jonsell, U., de Angelis, M., Boutron, C., Siggaard Andersen, M. L., Steffensen, J. P., Barbante, C., Gaspari, V.,			
	Gabrielli, P., and Wagenbach, D. Reconstruction of millennial changes in dust emission, transport and regional sea ice coverage			
910	using the deep EPICA ice cores from the Atlantic and Indian Ocean sector of Antarctica Earth and Planetary Science Letters			
710	asing the deep Latert with the Atlantic line inclining Sector of Atlantic Later until Latertary Sectice Letters			
	Francis, D., Eavrs, C., Cuesta, J., and Holland, D. Polar Cyclones at the Origin of the Reoccurrence of the Maud Rise Polynya			
	in Austral Winter 2017 Journal of Geophysical Research: Atmospheres 124 5251-5267, 2019.			
	Freer, J. J., Tarling, G. A., Collins, M. A., Partridge, J. C., and Genner, M. J., Predicting future distributions of lanternfish, a	-	Formatted	
915	significant ecological resource within the Southern Ocean Diversity and Distributions 25, 1259-1272,			
	https://doi.org/10.1111/ddi.12934_2019.		Formatted: German (Germany)	)
	Gilbert, E. and Holmes, Cz.: 2023's Antarctic sea ice extent is the lowest on record Weather, 79, 46-51,	—	Formatted	
	https://doi.org/10.1002/wea.4518,2024.		Formatted: German (Germany)	<u> </u>
	Goosse, H., Dalaiden, Q., Cavitte, M. G. P., and Zhang, L. Can we reconstruct the formation of large open ocean polynyas in	(	Formatted: Germany)	
920	the Southern Ocean using ice core records? Clim. Past 17:111-131, 2021.	(		
	Grieman, M. M., Nehrbass-Ahles, C., Hoffmann, H. M., Bauska, T. K., King, A. C. F., Mulvaney, R., Rhodes, R. H., Rowell, I. F., Thomas, E. R., and Wolff, E. W.: Abrupt Holocene ice loss due to thinning and ungrounding in the Weddell Sea	1	Formatted	()
	Embayment, Nature Geoscience, 17, 227-232, 10.1038/s41561-024-01375-8, 2024.	/		
	Gupta, M., Regan, H., Koo, Y., Chua, S. M. T., Li, X., and Heil, P.: Inferring the seasonality of sea ice floes in the Weddell			
925	Sea using ICESat-2, The Cryosphere, 19, 1241-1257, 10.5194/tc-19-1241-2025, 2025.			
123	Heaton, T. J., Köhler, P., Butzin, M., Bard, E., Reimer, R. W., Austin, W. E. N., Bronk Ramsey, C., Grootes, P. M., Hughen,	5	Formatted	
	K. A., Kromer, B., Reimer, P. J., Adkins, J., Burke, A., Cook, M. S., Olsen, J., and Skinner, L. C.:, Marine 20—The Marine	1	1 ormaccod	()
	Radiocarbon Age Calibration Curve (0-55,000 cal BP), Radiocarbon, 62, 779-820, 10.1017/RDC.2020.68, 2020.			
	Hillenbrand, C. D., Bentley, M. J., Stolldorf, T. D., Hein, A. S., Kuhn, G., Graham, A. G. C., Fogwill, C. J., Kristoffersen, Y.,			
930	Smith, J. A., Anderson, J. B., Larter, R. D., Melles, M., Hodgson, D. A., Mulvaney, R., and Sugden, D. E. Reconstruction of			
	changes in the Weddell Sea sector of the Antarctic Ice Sheet since the Last Glacial Maximum Quaternary Science Reviews			
	100 111 136, 2014.			

	Hillenbrand, CD., Smith, J. A., Hodell, D. A., Greaves, M., Poole, C. R., Kender, S., Williams, M., Andersen, T. J., Jernas,	-1	Formatted	(
	P. E., Elderfield, H., Klages, J. P., Roberts, S. J., Gohl, K., Larter, R. D., and Kuhn, G., West Antarctic Ice Sheet retreat driven	//		
935	by Holocene warm water incursions Nature \$47,43-48, 10.1038/nature22995, 2017.			
	Hiller, A., Wand, U., Kämpf, H., and Stackebrandt, W., Occupation of the Antarctic continent by petrels during the past 35	-	Formatted	(
	000 years: Inferences from a 14C study of stomach oil deposits, Polar Biology, 9, 69-77, 10.1007/BF00442032, 1988.			
	Hodell, D. A., Kanfoush, S. L., Shemesh, A., Crosta, X., Charles, C. D., and Guilderson, T. P.:. Abrupt Cooling of Antarctic	-	Formatted	
	Surface Waters and Sea Ice Expansion in the South Atlantic Sector of the Southern Ocean at 5000 cal yr B.P. Quaternary	//		
940	Research 56, 191-198, 10.1006/qres.2001.2252, 2001.			
	Hodgson, D. A. and Bentley, M. J. Lake highstands in the Pensacola Mountains and Shackleton Range 4300–2250 cal. yr	-	Formatted	(
	BP: Evidence of a warm climate anomaly in the interior of Antarctica, The Holocene, 23, 388-397, 10.1177/0959683612460790, 2013.			
	Hodgson, D. A., Hogan, K., Smith, J. M., Smith, J. A., Hillenbrand, C. D., Graham, A. G. C., Fretwell, P., Allen, C., Peck, V.,			
945	Arndt, J. E., Dorschel, B., Hübscher, C., Smith, A. M., and Larter, R. Deglaciation and future stability of the Coats Land ice			
	margin, Antarctica The Cryosphere 12 2383 2399, 2018.			
	Hodum, P. J. and Hobson, K. A.: Trophic relationships among Antarctic fulmarine petrels: insights into dietary overlap and			
	chick provisioning strategies inferred from stable-isotope ( $\delta^{15}N$ and $\delta^{13}C$ ) analyses, Marine Ecology Progress Series, 198, 273-			
	<u>281, 2000.</u>	,		
950	Holland, D. M.: Explaining the Weddell Polynyaa Large Ocean Eddy Shed at Maud Rise Science 292, 1697-1700,		Formatted	
	doi:10.1126/science.1059322, <b>2001</b> .			
	Honan, E. M., Wakefield, E. D., Phillips, R. A., Grecian, W. J., Prince, S., Robert, H., Descamps, S., Rix, A., Hoelzel, A. R.,			
	and McClymont, E. L.: The foraging distribution and habitat use of chick-rearing snow petrels from two colonies in Dronning			
055	Maud Land, Antarctica, Marine Biology, 172, 109, 10.1007/s00227-025-04657-w, 2025.			
955	Hückstädt, L. A., Koch, P. L., McDonald, B. I., Goebel, M. E., Crocker, D. E., and Costa, D. P.; Stable isotope analyses reveal	1	Formatted	(
	individual variability in the trophic ecology of a top marine predator, the southern elephant seal <u>a Oecologia</u> 169 <u>a 395-406</u> . 10.1007/s00442-011-2202-y, 2012.	//		
	Hughes, C., Johnson, M., von Glasow, R., Chance, R., Atkinson, H., Souster, T., Lee, G. A., Clarke, A., Meredith, M.,			
	Venables, H. J., Turner, S. M., Malin, G., and Liss, P. S. Climate induced change in biogenic bromine emissions from the			
960	Antarctic marine biosphere <i>Global Biogeochemical Cycles</i> 26 2012.			
900	Hutchings, J. K., Heil, P., Steer, A., and Hibler III, W. D.: Subsynoptic scale spatial variability of sea ice deformation in the			
	western Weddell Sea during early summer, Journal of Geophysical Research: Oceans, 117,			
	https://doi.org/10.1029/2011JC006961, 2012.			
	Imber, M. J.: The Origin of Petrel Stomach Oils: A Review The Condor, 78, 366-369, 10.2307/1367697, 1976.	اسا	Formatted	
965	Ionita, M., Large-scale drivers of the exceptionally low winter Antarctic sea ice extent in 2023, Frontiers in Earth Science, 12			
, 00	.10.3389/feart_2024.1333706, 2024.		Formatted	(
	Jena, B. and Pillai, A. N., Satellite observations of unprecedented phytoplankton blooms in the Maud Rise polynya, Southern		Formatted	(
	Ocean, The Cryosphere, 14, 1385-1398, 10.5194/tc-14-1385-2020, 2020.	/		(
	Jena, B., Ravichandran, M., and Turner, J. Recent Reoccurrence of Large Open Ocean Polynya on the Maud Rise Seamount			
970	Geophysical Research Letters 46 4320 4329, 2019.			
	Johnson, J. S., Nichols, K. A., Goehring, B. M., Balco, G., and Schaefer, J. Mr., Abrupt mid-Holocene ice loss in the western	_	Formatted	(···
	Weddell Sea Embayment of Antarctica, Earth and Planetary Science Letters, 518, 127-135,			(
	2019.https://doi.org/10.1016/j.epsl.2019.05.002, 2019		Formatted: German (Germany)	
	Johnson, K. M., McKay, R. M., Etourneau, J., Jiménez-Espejo, F. J., Albot, A., Riesselman, C. R., Bertler, N. A. N., Horgan,	,		
975	H. J., Crosta, X., Bendle, J., Ashley, K. E., Yamane, M., Yokoyama, Y., Pekar, S. F., Escutia, C., and Dunbar, R. B.: Sensitivity			
	of Holocene East Antarctic productivity to subdecadal variability set by sea ice, Nature Geoscience, 14, 762-768,			
	10.1038/s41561-021-00816-y, 2021.			
	Ju, SJ. and Harvey, H. R.: Lipids as markers of nutritional condition and diet in the Antarctic krill Euphausia superba and	-	Formatted	(
	Euphausia crystallorophias during austral winter Deep Sea Research Part II: Topical Studies in Oceanography 51, 2199-2214,	/		
980	https://doi.org/10.1016/j.dsr2.2004.08.004_2004.		Formatted: German (Germany)	
	Juckes, L.: The geology of north-eastern Heimefrontfjella, Dronning Maud Land, British Antarctic Survey1972.			

	Juggins, S.: rioja: Analysis of Quaternary Science Data. R package version 0.9-26, University of Newcastle, Newcastle upon		Formatted	
	Tyne, 2020.			
005	Kang, M., Fajaryanti, R., Son, W., Kim, J. H., and La, H. S. Acoustic Detection of Krill Scattering Layer in the Terra Nova			
985	Bay Polynya, Antarctica Frontiers in Marine Science 7 2020.			
	Knorr, G. and Lohmann, G. Southern Ocean origin for the resumption of Atlantic thermohaline circulation during deglaciation			
	Nature 424-532-536, 2003.			
	Kemeny, P. C., Kast, E. R., Hain, M. P., Fawcett, S. E., Fripiat, F., Studer, A. S., Martínez-García, A., Haug, G. H., and			
	Sigman, D. M.: A Seasonal Model of Nitrogen Isotopes in the Ice Age Antarctic Zone: Support for Weakening of the Southern			
990	Ocean Upper Overturning Cell, Paleoceanography and Paleoclimatology, 33, 1453-1471,			
	https://doi.org/10.1029/2018PA003478, 2018.			
	Kyrmanidou, A., Vadman, K. J., Ishman, S. E., Leventer, A., Brachfeld, S., Domack, E. W., and Wellner, J. Sz., Late Holocene	-	Formatted	
	oceanographic and climatic variability recorded by the Perseverance Drift, northwestern Weddell Sea, based on benthic			
	foraminifera and diatoms, Marine Micropaleontology, 141, 10-22, https://doi.org/10.1016/j.marmicro.2018.03.001, 2018.		Formatted: German (Germany)	
995	La, H. S., Lee, H., Fielding, S., Kang, D., Ha, H. K., Atkinson, A., Park, J., Siegel, V., Lee, S., and Shin, H. C. High density			
	of ice krill (Euphausia crystallorophias) in the Amundsen sea coastal polynya, Antarctica Deep Sea Research Part I:			
	Oceanographic Research Papers 95 75-84, 2015.			
	Laskar, J., Robutel, P., Joutel, F., Gastineau, M., Correia, A. C. M., and Levrard, B., Along-term numerical solution for the	_	Formatted	<u></u>
	insolation quantities of the Earth-, A&A&A, 428, 261-285, 2004.			
1000	Lewis, R. Wr. Studies of the glyceryl ethers of the stomach oil of Leach's petrel Oceanodroma leucorhoa (Viellot))	_	Formatted	
	Comparative Biochemistry and Physiology 19, 363-377, https://doi.org/10.1016/0010-406X(66)90147-2, 1966.	/	Formatted: German (Germany)	
	Lewis, R. Wr. Studies on the stomach oils of marine animals—II. Oils of some procellariiform birds Comparative		, ,,	
	Biochemistry and Physiology 31, 725-731, https://doi.org/10.1016/0010-406X(69)92072-6, 1969.		Formatted	(
	Liu, S., Liu, Y., Teschke, K., Hindell, M. A., Downey, R., Woods, B., Kang, B., Ma, S., Zhang, C., Li, J., Ye, Z., Sun, P., He,		Formatted: German (Germany)	
1005	J., and Tian, Y.: Incorporating mesopelagic fish into the evaluation of conservation areas for marine living resources under		Formatted	· · ·
	climate change scenarios, Marine Life Science & Technology, 6, 68-83, 10.1007/s42995-023-00188-9, 2024.		Tormutted	(
	Liu, X., Sun, L., Xie, Z., Yin, X., and Wang, Y., A 1300-year Record of Penguin Populations at Ardley Island in the Antarctic,	1	Formatted	(
	as Deduced from the Geochemical Data in the Ornithogenic Lake Sediments, Arctic, Antarctic, and Alpine Research, 37, 490-	//		
	498, 10.1657/1523-0430(2005)037[0490:AYROPP]2.0.CO;2 <b>, 2005</b> .			
1010	Macko, S. A. and Estep, M. L. F.: Microbial alteration of stable nitrogen and carbon isotopic compositions of organic matter.			
	Organic Geochemistry, 6, 787-790, https://doi.org/10.1016/0146-6380(84)90100-1, 1984.			
	Majewski, W. and Anderson, J. Br.: Holocene foraminiferal assemblages from Firth of Tay, Antarctic Peninsula: Paleoclimate	_	Formatted	
	implications, Marine Micropaleontology, 73, 135-147, https://doi.org/10.1016/j.marmicro.2009.08.003, 2009.		Formatted: German (Germany)	
	Martínez-Garcia, A., Rosell-Melé, A., Jaccard, S. L., Geibert, W., Sigman, D. M., and Haug, G. H. Southern Ocean dust-		Tormatean cerman (cermany)	
1015	climate coupling over the past four million years Nature 476 312 315, 2011.			
	Martínez-Garcia, A., Rosell-Melé, A., Geibert, W., Gersonde, R., Masqué, P., Gaspari, V., and Barbante, C. Links between			
	iron supply, marine productivity, sea surface temperature, and CO2 over the last 1.1 Ma Paleoceanography 24 2009.			
	Masson-Delmotte, V., Buiron, D., Ekaykin, A., Frezzotti, M., Gallée, H., Jouzel, J., Krinner, G., Landais, A., Motoyama, H.,	-1	Formatted	(
	Oerter, H., Pol, K., Pollard, D., Ritz, C., Schlosser, E., Sime, L. C., Sodemann, H., Stenni, B., Uemura, R., and Vimeux, F.	///		
1020	A comparison of the present and last interglacial periods in six Antarctic ice cores Clim. Past 7, 397-423, 10.5194/cp-7-397-	//		
	2011 <sub>e</sub> 2011.			
	McBride, M. M., Schram Stokke, O., Renner, A. H. H., Krafft, B. A., Bergstad, O. A., Biuw, M., Lowther, A. D., and Stiansen,			
	J. E.:. Antarctic krill Euphausia superba: spatial distribution, abundance, and management of fisheries in a changing climate.	_	Formatted	
	Marine Ecology Progress Series 668 185-214, 2021.			(
1025	McClymont, E. L., Bentley, M. J., Hodgson, D. A., Spencer-Jones, C. L., Wardley, T., West, M. D., Croudace, I. W., Berg,			
	S., Gröcke, D. R., Kuhn, G., Jamieson, S. S. R., Sime, L., and Phillips, R. A.: Summer sea-ice variability on the Antarctic	1	Formatted	[
	margin during the last glacial period reconstructed from snow petrel (Pagodroma nivea) stomach-oil deposits_Clim. Past_18_	//		
	381-403 <u>, 10.5194/cp-18-381-2022</u> <b>, 2022</b> .			
	Mezgec, K., Stenni, B., Crosta, X., Masson-Delmotte, V., Baroni, C., Braida, M., Ciardini, V., Colizza, E., Melis, R., Salvatore,			
1030	M. C., Severi, M., Scarchilli, C., Traversi, R., Udisti, R., and Frezzotti, M.: Holocene sea ice variability driven by wind and			
	polynya efficiency in the Ross Sea, Nature Communications, 8, 1334, 10.1038/s41467-017-01455-x, 2017.			

	Michalchuk, B. R., Anderson, J. B., Wellner, J. S., Manley, P. L., Majewski, W., and Bohaty, S., Holocene climate and glacial	1	Formatted	(
	history of the northeastern Antarctic Peninsula: the marine sedimentary record from a long SHALDRIL core Quaternary	//		
	Science Reviews, 28, 3049-3065, https://doi.org/10.1016/j.quascirev.2009.08.012, 2009.		Formatted: German (Germany)	
1035	Mulvaney, R., Abram, N. J., Hindmarsh, R. C. A., Arrowsmith, C., Fleet, L., Triest, J., Sime, L. C., Alemany, O., and Foord,			
	S. Recent Antarctic Peninsula warming relative to Holocene climate and ice-shelf history, Nature, 489, 141-144,	_	Formatted	(
	10.1038/nature11391, 2012.			· ·
	Nichols, K. A., Goehring, B. M., Balco, G., Johnson, J. S., Hein, A. S., and Todd, C.: New Last Glacial Maximum ice thickness	-	Formatted	(
	constraints for the Weddell Sea Embayment, Antarctica The Cryosphere 13, 2935-2951, 10.5194/tc-13-2935-2019, 2019,			
1040	Nie, S., Xiao, W., and Wang, R., Mid-Late Holocene climate variabilities in the Bransfield Strait, Antarctic Peninsula driven	-	Formatted	(
	by insolation and ENSO activities, Palaeogeography, Palaeoclimatology, Palaeoecology, 601, 111140,			
	https://doi.org/10.1016/j.palaeo.2022.111140_2022.		Formatted: German (Germany)	
	Nielsen, S. H. H., Koç, N. n., and Crosta, X.: Holocene climate in the Atlantic sector of the Southern Ocean: Controlled by			
	insolation or oceanic circulation?, Geology, 32, 317-320, 10.1130/g20334.1, 2004.			
1045	Nielsen, S. H. H., Hodell, D. A., Kamenov, G., Guilderson, T., and Perfit, M. R., Origin and significance of ice-rafted detritus	-	Formatted	
	in the Atlantic sector of the Southern Ocean, Geochemistry, Geophysics, Geosystems, 8,			
	https://doi.org/10.1029/2007GC001618_2007.		Formatted: German (Germany)	
	Antarctic sea ice at near-record-low maximum extent for 2024, last access: 9 October 2024.			
	Perren, B. B., Hodgson, D. A., Roberts, S. J., Sime, L., Van Nieuwenhuyze, W., Verleyen, E., and Vyverman, W. Southward			
1050	migration of the Southern Hemisphere westerly winds corresponds with warming climate over centennial timescales			
	Communications Earth & Environment 1 58, 2020.			
	Peck, V. L., Allen, C. S., Kender, S., McClymont, E. L., and Hodgson, D. A.: Oceanographic variability on the West Antarctic			
	Peninsula during the Holocene and the influence of upper circumpolar deep water, Quaternary Science Reviews, 119, 54-65,			
	https://doi.org/10.1016/j.quascirev.2015.04.002, 2015.			
1055	Purich, A. and Doddridge, E. W. Record low Antarctic sea ice coverage indicates a new sea ice state Communications Earth	_	Formatted	
	& Environment, 4, 314, 10.1038/s43247-023-00961-9, 2023.			`
	Ran, Q., Duan, M., Wang, P., Ye, Z., Mou, J., Wang, X., Tian, Y., Zhang, C., Qiao, H., and Zhang, J., Predicting the current	-1	Formatted	(
	habitat suitability and future habitat changes of Antarctic jonasfish Notolepis coatsorum in the Southern Ocean, Deep Sea	//		
	Research Part II: Topical Studies in Oceanography 199, 105077, https://doi.org/10.1016/j.dsr2.2022.105077, 2022.		Formatted: German (Germany)	
1060	Rau, G. H., Ainley, D. G., Bengtson, J. L., Torres, J. J., and Hopkins, T. L., 15N/14N and 13C/12C in Weddell Sea birds, seals,		Formatted	(
	and fish: implications for diet and trophic structure Marine Ecology Progress Series, 84, 1-8, 1992.			
	Reisinger, R. R., Gröcke, D. R., Lübcker, N., McClymont, E. L., Hoelzel, A. R., and de Bruyn, P. J. N. 4 variation in the diet	-	Formatted	(
	of killer whales Orcinus orca at Marion Island, Southern Ocean Marine Ecology Progress Series 549 263-274, 2016.			
	Renssen, H., Goosse, H., Fichefet, T., Masson-Delmotte, V., and Koç, N.: Holocene climate evolution in the high-latitude	-1	Formatted	(
1065	Southern Hemisphere simulated by a coupled atmosphere-sea ice-ocean-vegetation model, The Holocene, 15, 951-964,	//		
	10.1191/0959683605hl869ra, 2005.			
	Rignot, E., J. Mouginot, and B. Scheuchl.: MEaSUREs Grounding Zone of the Antarctic Ice			
	Sheet, Version 1. [2018] [dataset], doi: 10.5067/HGLT8XB480E4, 2022.			
	Roberts, S. J., Monien, P., Foster, L. C., Loftfield, J., Hocking, E. P., Schnetger, B., Pearson, E. J., Juggins, S., Fretwell, P.,			
1070	Ireland, L., Ochyra, R., Haworth, A. R., Allen, C. S., Moreton, S. G., Davies, S. J., Brumsack, HJ., Bentley, M. J., and			
	Hodgson, D. A. Past penguin colony responses to explosive volcanism on the Antarctic Peninsula, Nature Communications,	_	Formatted	(
	8 <sub>4</sub> 14914, 10.1038/ncomms14914, 2017.			
	Rontani, JF. and Volkman, J. K Phytol degradation products as biogeochemical tracers in aquatic environments Organic	-	Formatted	(
	Geochemistry 34, 1-35, https://doi.org/10.1016/S0146-6380(02)00185-7, 2003.		Formatted: German (Germany)	
1075	Sargent, J. R. and Falk-Petersen, S-: Ecological investigations on the zooplankton community in balsfjorden, northern Norway:		Formatted	
1	Lipids and fatty acids in Meganyctiphanes norvegica, Thysanoessa raschi and T. inermis during mid-winter Mar. Biol62	/	romatted	

Formatted

131-137, 10.1007/BF00388175, 1981.
Sarmiento, J. L., Gruber, N., Brzezinski, M. A., and Dunne, J. P., High-latitude controls of thermocline nutrients and low latitude biological productivity, Nature, 427, 56-60, 10.1038/nature02127, 2004.

		-		
1080	Shatova, O., Wing, S. R., Gault-Ringold, M., Wing, L., and Hoffmann, L. J. Seabird guano enhances phytoplankton	-/	Formatted	
	production in the Southern Ocean Journal of Experimental Marine Biology and Ecology 483 74-87,			
	<del>2016.</del> https://doi.org/10.1016/j.jembe.2016.07.004, 2016,		Formatted: German (Germany)	J
	Shatova, O. A., Wing, S. R., Hoffmann, L. J., Wing, L. C., and Gault-Ringold, M., Phytoplankton community structure is		Formatted	
	influenced by seabird guano enrichment in the Southern Ocean, Estuarine, Coastal and Shelf Science, 191, 125-135,			
1085	<del>2017.</del> https://doi.org/10.1016/j.ecss.2017.04.021, 2017		Formatted: German (Germany)	J
	Sigman, D. M., Jaccard, S. L., and Haug, G. H. Polar ocean stratification in a cold climate <i>Nature</i> 428 59-63, 2004.			
	Smith, J. A., Hillenbrand, CD., Pudsey, C. J., Allen, C. S., and Graham, A. G. C., The presence of polynyas in the Weddell	1	Formatted	
	Sea during the Last Glacial Period with implications for the reconstruction of sea-ice limits and ice sheet history Earth and	//		
	Planetary Science Letters 296 287-298, https://doi.org/10.1016/j.epsl.2010.05.008 2010.		Formatted: German (Germany)	J
1090	Sparaventi, E., Rodríguez-Romero, A., Barbosa, A., Ramajo, L., and Tovar-Sánchez, A., Trace elements in Antarctic penguins	-	Formatted	
	and the potential role of guano as source of recycled metals in the Southern Ocean, Chemosphere, 285, 131423,			
	https://doi.org/10.1016/j.chemosphere.2021.131423_2021.		Formatted: German (Germany)	
	St John Glew, K., Espinasse, B., Hunt, B. P. V., Pakhomov, E. A., Bury, S. J., Pinkerton, M., Nodder, S. D., Gutiérrez-			
	Rodríguez, A., Safi, K., Brown, J. C. S., Graham, L., Dunbar, R. B., Mucciarone, D. A., Magozzi, S., Somes, C., and Trueman,	_		
1095	C. N. Lisoscape Models of the Southern Ocean: Predicting Spatial and Temporal Variability in Carbon and Nitrogen Isotope	1	Formatted	
	Compositions of Particulate Organic Matter Global Biogeochemical Cycles 35, e2020GB006901,	_		
	https://doi.org/10.1029/2020GB006901_2021.		Formatted: German (Germany)	
	Steig, E. J., Hart, C. P., White, J. W. C., Cunningham, W. L., Davis, M. D., and Saltzman, E. S. Changes in climate, ocean and			
4400	ice-sheet conditions in the Ross embayment, Antarctica, at 6 ka Annals of Glaciology 27 305-310, 1998.			
1100	Stefanova, M. and Disnar, J. R.: Composition and early diagenesis of fatty acids in lacustrine sediments, lake Aydat (France),			
	Organic Geochemistry, 31, 41-55, https://doi.org/10.1016/S0146-6380(99)00134-5, 2000.			
	Studer, A. S., Sigman, D. M., Martínez-García, A., Thöle, L. M., Michel, E., Jaccard, S. L., Lippold, J. A., Mazaud, A., Wang,			
	X. T., Robinson, L. F., Adkins, J. F., and Haug, G. H.: Increased nutrient supply to the Southern Ocean during the Holocene			
	and its implications for the pre-industrial atmospheric CO2 rise, Nature Geoscience, 11, 756-760, 10.1038/s41561-018-0191-			
1105	0.0010			
1105	8, 2018. Sup I Vio 7, and 7hoo I + A 2,000 year record of nanoppin namelations. Nature, 407, 959, 959, 10, 1039/25039162, 2000.			
1105	Sun, L., Xie, Z., and Zhao, J-:: A 3,000-year record of penguin populations, Nature, 407, 858-858, 10.1038/35038163, 2000.	(	Formatted	
1105	Sun, L., Xie, Z., and Zhao, J., A 3,000-year record of penguin populations Nature 407 858-858, 10.1038/35038163, 2000.  Tatur, A., Myrcha, A., and Niegodzisz, J., Formation of abandoned penguin rookery ecosystems in the maritime Antarctic	(	Formatted Formatted	
1105	Sun, L., Xie, Z., and Zhao, J., A 3,000-year record of penguin populations, Nature, 407, 858-858, 10.1038/35038163, 2000.  Tatur, A., Myrcha, A., and Niegodzisz, J., Formation of abandoned penguin rookery ecosystems in the maritime Antarctic, Polar Biology, 17, 405-417, 10.1007/s003000050135, 1997.	(	Formatted	
	Sun, L., Xie, Z., and Zhao, J., A 3,000-year record of penguin populations, Nature, 407, 858-858, 10.1038/35038163, 2000.  Tatur, A., Myrcha, A., and Niegodzisz, J., Formation of abandoned penguin rookery ecosystems in the maritime Antarctic Polar Biology, 17, 405-417, 10.1007/s003000050135, 1997.  Taylor, F., Whitehead, J., and Domack, E., Holocene paleoclimate change in the Antarctic Peninsula: evidence from the			
	Sun, L., Xie, Z., and Zhao, J.: A 3,000-year record of penguin populations, Nature, 407, 858-858, 10.1038/35038163, 2000.  Tatur, A., Myrcha, A., and Niegodzisz, J.: Formation of abandoned penguin rookery ecosystems in the maritime Antarctic Polar Biology, 17, 405-417, 10.1007/s003000050135, 1997.  Taylor, F., Whitehead, J., and Domack, E.: Holocene paleoclimate change in the Antarctic Peninsula: evidence from the diatom, sedimentary and geochemical record, Mar. Micropaleontol., 41, 25-43, https://doi.org/10.1016/S0377-		Formatted Formatted	
	Sun, L., Xie, Z., and Zhao, J.; A 3,000-year record of penguin populations, Nature, 407, 858-858, 10.1038/35038163, 2000. Tatur, A., Myrcha, A., and Niegodzisz, J.; Formation of abandoned penguin rookery ecosystems in the maritime Antarctic, Polar Biology, 17, 405-417, 10.1007/s003000050135, 1997. Taylor, F., Whitehead, J., and Domack, E.; Holocene paleoclimate change in the Antarctic Peninsula: evidence from the diatom, sedimentary and geochemical record, Mar. Micropaleontol., 41, 25-43, https://doi.org/10.1016/S0377-8398(00)00049-9, 2001.		Formatted Formatted: German (Germany)	
	Sun, L., Xie, Z., and Zhao, J.; A 3,000-year record of penguin populations, Nature, 407, 858-858, 10.1038/35038163, 2000.  Tatur, A., Myrcha, A., and Niegodzisz, J.; Formation of abandoned penguin rookery ecosystems in the maritime Antarctic, Polar Biology, 17, 405-417, 10.1007/s003000050135, 1997.  Taylor, F., Whitehead, J., and Domack, E.; Holocene paleoclimate change in the Antarctic Peninsula: evidence from the diatom, sedimentary and geochemical record, Mar. Micropaleontol., 41, 25-43, https://doi.org/10.1016/S0377-8398(00)00049-9, 2001.  Ter Braak, C. and Smilauer, P.; Canoco for Windows version 4.5, Biometris—Plant Research International, Wageningen, 2002.		Formatted Formatted	
	Sun, L., Xie, Z., and Zhao, J.; A 3,000-year record of penguin populations Nature 407 858-858, 10.1038/35038163, 2000.  Tatur, A., Myrcha, A., and Niegodzisz, J.; Formation of abandoned penguin rookery ecosystems in the maritime Antarctic Polar Biology, 17, 405-417, 10.1007/s003000050135, 1997.  Taylor, F., Whitehead, J., and Domack, E.; Holocene paleoclimate change in the Antarctic Peninsula: evidence from the diatom, sedimentary and geochemical record Mar. Micropaleontol., 41, 25-43, https://doi.org/10.1016/S0377-8398(00)00049-9, 2001.  Ter Braak, C. and Smilauer, P.; Canoco for Windows version 4.5, Biometris—Plant Research International, Wageningen, 2002.  Totten, R. L., Anderson, J. B., Fernandez, R., and Wellner, J. S.; Marine record of Holocene climate, ocean, and cryosphere		Formatted Formatted: German (Germany)	
1110	Sun, L., Xie, Z., and Zhao, J.; A 3,000-year record of penguin populations, Nature, 407, 858-858, 10.1038/35038163, 2000.  Tatur, A., Myrcha, A., and Niegodzisz, J.; Formation of abandoned penguin rookery ecosystems in the maritime Antarctic, Polar Biology, 17, 405-417, 10.1007/s003000050135, 1997.  Taylor, F., Whitehead, J., and Domack, E.; Holocene paleoclimate change in the Antarctic Peninsula: evidence from the diatom, sedimentary and geochemical record, Mar. Micropaleontol., 41, 25-43, https://doi.org/10.1016/S0377-8398(00)00049-9, 2001.  Ter Braak, C. and Smilauer, P.; Canoco for Windows version 4.5, Biometris—Plant Research International, Wageningen, 2002.  Totten, R. L., Anderson, J. B., Fernandez, R., and Wellner, J. S.; Marine record of Holocene climate, ocean, and cryosphere interactions: Herbert Sound, James Ross Island, Antarctica, Quaternary Science Reviews, 129, 239-259,		Formatted Formatted: German (Germany) Formatted Formatted	
	Sun, L., Xie, Z., and Zhao, J.; A 3,000-year record of penguin populations, Nature, 407, 858-858, 10.1038/35038163, 2000.  Tatur, A., Myrcha, A., and Niegodzisz, J.; Formation of abandoned penguin rookery ecosystems in the maritime Antarctic Polar Biology, 17, 405-417, 10.1007/s003000050135, 1997.  Taylor, F., Whitehead, J., and Domack, E.; Holocene paleoclimate change in the Antarctic Peninsula: evidence from the diatom, sedimentary and geochemical record Mar. Micropaleontol., 41, 25-43, https://doi.org/10.1016/S0377-8398(00)00049-9, 2001.  Ter Braak, C. and Smilauer, P.; Canoco for Windows version 4.5, Biometris—Plant Research International, Wageningen, 2002. Totten, R. L., Anderson, J. B., Fernandez, R., and Wellner, J. S.; Marine record of Holocene climate, ocean, and cryosphere interactions: Herbert Sound, James Ross Island, Antarctica, Quaternary Science Reviews, 129, 239-259, https://doi.org/10.1016/j.quascirev.2015.09.009, 2015.		Formatted  Formatted: German (Germany)  Formatted	
1110	Sun, L., Xie, Z., and Zhao, J.; A 3,000-year record of penguin populations, Nature, 407, 858-858, 10.1038/35038163, 2000. Tatur, A., Myrcha, A., and Niegodzisz, J.; Formation of abandoned penguin rookery ecosystems in the maritime Antarctic, Polar Biology, 17, 405-417, 10.1007/s003000050135, 1997. Taylor, F., Whitehead, J., and Domack, E.; Holocene paleoclimate change in the Antarctic Peninsula: evidence from the diatom, sedimentary and geochemical record, Mar. Micropaleontol., 41, 25-43, https://doi.org/10.1016/S0377-8398(00)00049-9, 2001.  Ter Braak, C. and Smilauer, P.; Canoco for Windows version 4.5, Biometris—Plant Research International, Wageningen, 2002. Totten, R. L., Anderson, J. B., Fernandez, R., and Wellner, J. S.; Marine record of Holocene climate, ocean, and cryosphere interactions: Herbert Sound, James Ross Island, Antarctica, Quaternary Science Reviews, 129, 239-259, https://doi.org/10.1016/j.quascirev.2015.09.009, 2015.  Turner, J., Guarino, M. V., Arnatt, J., Jena, B., Marshall, G. J., Phillips, T., Bajish, C. C., Clem, K., Wang, Z., Andersson, T.,		Formatted  Formatted: German (Germany)  Formatted  Formatted  Formatted  Formatted: German (Germany)	
1110	Sun, L., Xie, Z., and Zhao, J.; A 3,000-year record of penguin populations, Nature, 407, 858-858, 10.1038/35038163, 2000. Tatur, A., Myrcha, A., and Niegodzisz, J.; Formation of abandoned penguin rookery ecosystems in the maritime Antarctic, Polar Biology, 17, 405-417, 10.1007/s003000050135, 1997.  Taylor, F., Whitehead, J., and Domack, E.; Holocene paleoclimate change in the Antarctic Peninsula: evidence from the diatom, sedimentary and geochemical record, Mar. Micropaleontol., 41, 25-43, https://doi.org/10.1016/S0377-8398(00)00049-9, 2001.  Ter Braak, C. and Smilauer, P.; Canoco for Windows version 4.5, Biometris-Plant Research International, Wageningen, 2002.  Totten, R. L., Anderson, J. B., Fernandez, R., and Wellner, J. S.; Marine record of Holocene climate, ocean, and cryosphere interactions: Herbert Sound, James Ross Island, Antarctica, Quaternary Science Reviews, 129, 239-259, https://doi.org/10.1016/j.quascirev.2015.09.009, 2015.  Turner, J., Guarino, M. V., Arnatt, J., Jena, B., Marshall, G. J., Phillips, T., Bajish, C. C., Clem, K., Wang, Z., Andersson, T., Murphy, E. J., and Cavanagh, R.; Recent Decrease of Summer Sea Ice in the Weddell Sea, Antarctica, Geophysical Research		Formatted  Formatted: German (Germany)  Formatted  Formatted  Formatted  Formatted: German (Germany)  Formatted: German (Germany)	
1110	Sun, L., Xie, Z., and Zhao, J.; A 3,000-year record of penguin populations, Nature, 407, 858-858, 10.1038/35038163, 2000. Tatur, A., Myrcha, A., and Niegodzisz, J.; Formation of abandoned penguin rookery ecosystems in the maritime Antarctic, Polar Biology, 17, 405-417, 10.1007/s003000050135, 1997.  Taylor, F., Whitehead, J., and Domack, E.; Holocene paleoclimate change in the Antarctic Peninsula: evidence from the diatom, sedimentary and geochemical record, Mar. Micropaleontol., 41, 25-43, https://doi.org/10.1016/S0377-8398(00)00049-9, 2001.  Ter Braak, C. and Smilauer, P.; Canoco for Windows version 4.5, Biometris—Plant Research International, Wageningen, 2002.  Totten, R. L., Anderson, J. B., Fernandez, R., and Wellner, J. S.; Marine record of Holocene climate, ocean, and cryosphere interactions: Herbert Sound, James Ross Island, Antarctica, Quaternary Science Reviews, 129, 239-259, https://doi.org/10.1016/j.quascirev.2015.09.009, 2015.  Turner, J., Guarino, M. V., Arnatt, J., Jena, B., Marshall, G. J., Phillips, T., Bajish, C. C., Clem, K., Wang, Z., Andersson, T., Murphy, E. J., and Cavanagh, R.; Recent Decrease of Summer Sea Ice in the Weddell Sea, Antarctica, Geophysical Research Letters, 47, e2020GL087127, https://doi.org/10.1029/2020GL087127, 2020.		Formatted  Formatted: German (Germany)  Formatted  Formatted  Formatted  Formatted: German (Germany)	
1110	Sun, L., Xie, Z., and Zhao, J.; A 3,000-year record of penguin populations, Nature, 407, 858-858, 10.1038/35038163, 2000. Tatur, A., Myrcha, A., and Niegodzisz, J.; Formation of abandoned penguin rookery ecosystems in the maritime Antarctic, Polar Biology, 17, 405-417, 10.1007/s003000050135, 1997.  Taylor, F., Whitehead, J., and Domack, E.; Holocene paleoclimate change in the Antarctic Peninsula: evidence from the diatom, sedimentary and geochemical record, Mar. Micropaleontol., 41, 25-43, https://doi.org/10.1016/S0377-8398(00)00049-9, 2001.  Ter Braak, C. and Smilauer, P.; Canoco for Windows version 4.5, Biometris—Plant Research International, Wageningen, 2002.  Totten, R. L., Anderson, J. B., Fernandez, R., and Wellner, J. S.; Marine record of Holocene climate, ocean, and cryosphere interactions: Herbert Sound, James Ross Island, Antarctica, Quaternary Science Reviews, 129, 239-259, https://doi.org/10.1016/j.quascirev.2015.09.009, 2015.  Turner, J., Guarino, M. V., Arnatt, J., Jena, B., Marshall, G. J., Phillips, T., Bajish, C. C., Clem, K., Wang, Z., Andersson, T., Murphy, E. J., and Cavanagh, R.; Recent Decrease of Summer Sea Ice in the Weddell Sea, Antarctica, Geophysical Research Letters, 47, e2020GL087127, https://doi.org/10.1029/2020GL087127, 2020.  Valenzuela, L. O., Rowntree, V. J., Sironi, M., and Seger, J.; Stable isotopes (§ 15N, § 13C, § 34S) in skin reveal diverse food		Formatted  Formatted: German (Germany)  Formatted  Formatted  Formatted  Formatted: German (Germany)  Formatted: German (Germany)	
1110	Sun, L., Xie, Z., and Zhao, J.; A 3,000-year record of penguin populations, Nature, 407, 858-858, 10.1038/35038163, 2000. Tatur, A., Myrcha, A., and Niegodzisz, J.; Formation of abandoned penguin rookery ecosystems in the maritime Antarctic, Polar Biology, 17, 405-417, 10.1007/s003000050135, 1997.  Taylor, F., Whitehead, J., and Domack, E.; Holocene paleoclimate change in the Antarctic Peninsula: evidence from the diatom, sedimentary and geochemical record, Mar. Micropaleontol., 41, 25-43, https://doi.org/10.1016/S0377-8398(00)00049-9, 2001.  Ter Braak, C. and Smilauer, P.; Canoco for Windows version 4.5, Biometris—Plant Research International, Wageningen, 2002.  Totten, R. L., Anderson, J. B., Fernandez, R., and Wellner, J. S.; Marine record of Holocene climate, ocean, and cryosphere interactions: Herbert Sound, James Ross Island, Antarctica, Quaternary Science Reviews, 129, 239-259, https://doi.org/10.1016/j.quascirev.2015.09.009, 2015.  Turner, J., Guarino, M. V., Arnatt, J., Jena, B., Marshall, G. J., Phillips, T., Bajish, C. C., Clem, K., Wang, Z., Andersson, T., Murphy, E. J., and Cavanagh, R.; Recent Decrease of Summer Sea Ice in the Weddell Sea, Antarctica, Geophysical Research Letters, 47, e2020GL087127, https://doi.org/10.1029/2020GL087127, 2020.  Valenzuela, L. O., Rowntree, V. J., Sironi, M., and Seger, J.; Stable isotopes (§15N, §13C, §34S) in skin reveal diverse food sources used by southern right whales Eubalaena australis, Marine Ecology Progress Series, 603, 243-255, 2018.		Formatted  Formatted: German (Germany)  Formatted  Formatted  Formatted  Formatted: German (Germany)  Formatted  Formatted  Formatted: German (Germany)	
1110	Sun, L., Xie, Z., and Zhao, J.; A 3,000-year record of penguin populations, Nature, 407, 858-858, 10.1038/35038163, 2000. Tatur, A., Myrcha, A., and Niegodzisz, J.; Formation of abandoned penguin rookery ecosystems in the maritime Antarctic, Polar Biology, 17, 405-417, 10.1007/s003000050135, 1997.  Taylor, F., Whitehead, J., and Domack, E.; Holocene paleoclimate change in the Antarctic Peninsula: evidence from the diatom, sedimentary and geochemical record, Mar. Micropaleontol., 41, 25-43, https://doi.org/10.1016/S0377-8398(00)00049-9, 2001.  Ter Braak, C. and Smilauer, P.; Canoco for Windows version 4.5, Biometris—Plant Research International, Wageningen, 2002.  Totten, R. L., Anderson, J. B., Fernandez, R., and Wellner, J. S.; Marine record of Holocene climate, ocean, and cryosphere interactions: Herbert Sound, James Ross Island, Antarctica, Quaternary Science Reviews, 129, 239-259, https://doi.org/10.1016/j.quascirev.2015.09.009, 2015.  Turner, J., Guarino, M. V., Arnatt, J., Jena, B., Marshall, G. J., Phillips, T., Bajish, C. C., Clem, K., Wang, Z., Andersson, T., Murphy, E. J., and Cavanagh, R.; Recent Decrease of Summer Sea Ice in the Weddell Sea, Antarctica, Geophysical Research Letters, 47, e2020GL087127, https://doi.org/10.1029/2020GL087127, 2020.  Valenzuela, L. O., Rowntree, V. J., Sironi, M., and Seger, J.; Stable isotopes (8 <sup>15</sup> N, 8 <sup>13</sup> C, 8 <sup>34</sup> S) in skin reveal diverse food sources used by southern right whales Eubalaena australis, Marine Ecology Progress Series, 603, 243-255, 2018.  van den Berg, G. L., Vermeulen, E., Valenzuela, L. O., Bérubé, M., Ganswindt, A., Gröcke, D. R., Hall, G., Hulva, P.,		Formatted  Formatted: German (Germany)  Formatted  Formatted  Formatted: German (Germany)  Formatted  Formatted: German (Germany)  Formatted: German (Germany)	
1110	Sun, L., Xie, Z., and Zhao, J.; A 3,000-year record of penguin populations, Nature, 407, 858-858, 10.1038/35038163, 2000. Tatur, A., Myrcha, A., and Niegodzisz, J.; Formation of abandoned penguin rookery ecosystems in the maritime Antarctic, Polar Biology, 17, 405-417, 10.1007/s003000050135, 1997.  Taylor, F., Whitehead, J., and Domack, E.; Holocene paleoclimate change in the Antarctic Peninsula: evidence from the diatom, sedimentary and geochemical record, Mar. Micropaleontol., 41, 25-43, https://doi.org/10.1016/S0377-8398(00)00049-9, 2001.  Ter Braak, C. and Smilauer, P.; Canoco for Windows version 4.5, Biometris-Plant Research International, Wageningen, 2002. Totten, R. L., Anderson, J. B., Fernandez, R., and Wellner, J. S.; Marine record of Holocene climate, ocean, and cryosphere interactions: Herbert Sound, James Ross Island, Antarctica, Quaternary Science Reviews, 129, 239-259, https://doi.org/10.1016/j.quascirev.2015.09.009, 2015.  Turner, J., Guarino, M. V., Arnatt, J., Jena, B., Marshall, G. J., Phillips, T., Bajish, C. C., Clem, K., Wang, Z., Andersson, T., Murphy, E. J., and Cavanagh, R.; Recent Decrease of Summer Sea Ice in the Weddell Sea, Antarctica, Geophysical Research Letters, 47, e2020GL087127, https://doi.org/10.1029/2020GL087127, 2020.  Valenzuela, L. O., Rowntree, V. J., Sironi, M., and Seger, J.; Stable isotopes (δ15N, δ13C, δ34S) in skin reveal diverse food sources used by southern right whales Eubalaena australis, Marine Ecology Progress Series, 603, 243-255, 2018.  van den Berg, G. L., Vermeulen, E., Valenzuela, L. O., Bérübé, M., Ganswindt, A., Gröcke, D. R., Hall, G., Hulva, P., Neveceralova, P., Palsbøll, P. J., and Carroll, E. L.; Decadal shift in foraging strategy of a migratory southern ocean predator.		Formatted  Formatted: German (Germany)  Formatted  Formatted  Formatted: German (Germany)  Formatted  Formatted  Formatted: German (Germany)  Formatted  Formatted  Formatted	
1110	Sun, L., Xie, Z., and Zhao, J.; A 3,000-year record of penguin populations Nature 407 \$58-858, 10.1038/35038163, 2000. Tatur, A., Myrcha, A., and Niegodzisz, J.; Formation of abandoned penguin rookery ecosystems in the maritime Antarctic Polar Biology, 17, 405-417, 10.1007/s003000050135, 1997.  Taylor, F., Whitehead, J., and Domack, E.; Holocene paleoclimate change in the Antarctic Peninsula: evidence from the diatom, sedimentary and geochemical record Mar. Micropaleontol., 41, 25-43, https://doi.org/10.1016/S0377-8398(00)00049-9, 2001.  Ter Braak, C. and Smilauer, P.; Canoco for Windows version 4.5 Biometris-Plant Research International, Wageningen, 2002. Totten, R. L., Anderson, J. B., Fernandez, R., and Wellner, J. S.; Marine record of Holocene climate, ocean, and cryosphere interactions: Herbert Sound, James Ross Island, Antarctica, Quaternary Science Reviews, 129, 239-259, https://doi.org/10.1016/j.quascirev.2015.09.009, 2015.  Turner, J., Guarino, M. V., Arnatt, J., Jena, B., Marshall, G. J., Phillips, T., Bajish, C. C., Clem, K., Wang, Z., Andersson, T., Murphy, E. J., and Cavanagh, R.; Recent Decrease of Summer Sea Ice in the Weddell Sea, Antarctica, Geophysical Research Letters, 47, e2020GL087127, https://doi.org/10.1029/2020GL087127, 2020.  Valenzuela, L. O., Rowntree, V. J., Sironi, M., and Seger, J.; Stable isotopes (δ15N, δ13C, δ34S) in skin reveal diverse food sources used by southern right whales Eubalaena australis, Marine Ecology Progress Series, 603, 243-255, 2018.  van den Berg, G. L., Vermeulen, E., Valenzuela, L. O., Bérubé, M., Ganswindt, A., Gröcke, D. R., Hall, G., Hulva, P., Neveceralova, P., Palsbøll, P. J., and Carroll, E. L.; Decadal shift in foraging strategy of a migratory southern ocean predator, Global Change Biology, 27, 1052-1067, https://doi.org/10.1111/gcb.15465, 2021.		Formatted  Formatted: German (Germany)  Formatted  Formatted  Formatted: German (Germany)  Formatted  Formatted: German (Germany)  Formatted: German (Germany)	
1110 1115 1120	Sun, L., Xie, Z., and Zhao, J.; A 3,000-year record of penguin populations, Nature, 407, 858-858, 10.1038/35038163, 2000. Tatur, A., Myrcha, A., and Niegodzisz, J.; Formation of abandoned penguin rookery ecosystems in the maritime Antarctic, Polar Biology, 17, 405-417, 10.1007/s003000050135, 1997.  Taylor, F., Whitehead, J., and Domack, E.; Holocene paleoclimate change in the Antarctic Peninsula: evidence from the diatom, sedimentary and geochemical record, Mar. Micropaleontol., 41, 25-43, https://doi.org/10.1016/S0377-8398(00)00049-9, 2001.  Ter Braak, C. and Smilauer, P.; Canoco for Windows version 4.5, Biometris—Plant Research International, Wageningen, 2002.  Totten, R. L., Anderson, J. B., Fernandez, R., and Wellner, J. S.; Marine record of Holocene climate, ocean, and cryosphere interactions: Herbert Sound, James Ross Island, Antarctica, Quaternary Science Reviews, 129, 239-259, https://doi.org/10.1016/j.quascirev.2015.09.009, 2015.  Turner, J., Guarino, M. V., Arnatt, J., Jena, B., Marshall, G. J., Phillips, T., Bajish, C. C., Clem, K., Wang, Z., Andersson, T., Murphy, E. J., and Cavanagh, R.; Recent Decrease of Summer Sea Ice in the Weddell Sea, Antarctica, Geophysical Research Letters, 47, e2020GL087127, https://doi.org/10.1029/2020GL087127, 2020.  Valenzuela, L. O., Rowntree, V. J., Sironi, M., and Seger, J.; Stable isotopes (815N, 813C, 834S) in skin reveal diverse food sources used by southern right whales Eubalaena australis, Marine Ecology Progress Series, 603, 243-255, 2018.  van den Berg, G. L., Vermeulen, E., Valenzuela, L. O., Bérubé, M., Ganswindt, A., Gröcke, D. R., Hall, G., Hulva, P., Neveceralova, P., Palsbøll, P. J., and Carroll, E. L.; Decadal shift in foraging strategy of a migratory southern ocean predator, Global Change Biology, 27, 1052-1067, https://doi.org/10.1111/gcb.15465, 2021.  Verleyen, E., Hodgson, D. A., Sabbe, K., Cremer, H., Emslie, S. D., Gibson, J., Hall, B., Imura, S., Kudoh, S., Marshall, G.		Formatted  Formatted: German (Germany)  Formatted  Formatted  Formatted: German (Germany)  Formatted  Formatted  Formatted: German (Germany)  Formatted  Formatted  Formatted	
1110 1115 1120	Sun, L., Xie, Z., and Zhao, J.; A 3,000-year record of penguin populations, Nature, 407, 858-858, 10.1038/35038163, 2000. Tatur, A., Myrcha, A., and Niegodzisz, J.; Formation of abandoned penguin rookery ecosystems in the maritime Antarctic, Polar Biology, 17, 405-417, 10.1007/s003000050135, 1997.  Taylor, F., Whitehead, J., and Domack, E.; Holocene paleoclimate change in the Antarctic Peninsula: evidence from the diatom, sedimentary and geochemical record, Mar. Micropaleontol., 41, 25-43, https://doi.org/10.1016/S0377-8398(00)00049-9, 2001.  Ter Braak, C. and Smilauer, P.; Canoco for Windows version 4.5, Biometris—Plant Research International, Wageningen, 2002.  Totten, R. L., Anderson, J. B., Fernandez, R., and Wellner, J. S.; Marine record of Holocene climate, ocean, and cryosphere interactions: Herbert Sound, James Ross Island, Antarctica, Quaternary Science Reviews, 129, 239-259, https://doi.org/10.1016/j.quascirev.2015.09.009, 2015.  Turner, J., Guarino, M. V., Arnatt, J., Jena, B., Marshall, G. J., Phillips, T., Bajish, C. C., Clem, K., Wang, Z., Andersson, T., Murphy, E. J., and Cavanagh, R.; Recent Decrease of Summer Sea Ice in the Weddell Sea, Antarctica, Geophysical Research Letters, 47, e2020GL087127, https://doi.org/10.1029/2020GL087127, 2020.  Valenzuela, L. O., Rowntree, V. J., Sironi, M., and Seger, J.; Stable isotopes (815N, 813C, 834S) in skin reveal diverse food sources used by southern right whales Eubalaena australis, Marine Ecology Progress Series, 603, 243-255, 2018.  van den Berg, G. L., Vermeulen, E., Valenzuela, L. O., Bérubé, M., Ganswindt, A., Gröcke, D. R., Hall, G., Hulva, P., Neveceralova, P., Palsbøll, P. J., and Carroll, E. L.; Decadal shift in foraging strategy of a migratory southern ocean predator, Global Change Biology, 27, 1052-1067, https://doi.org/10.1111/gcb.15465, 2021.  Verleyen, E., Hodgson, D. A., Sabbe, K., Cremer, H., Emslie, S. D., Gibson, J., Hall, B., Imura, S., Kudoh, S., Marshall, G. J., McMinn, A., Melles, M., Newman, L., Roberts, D., Roberts, S. J., Singh, S		Formatted  Formatted: German (Germany)  Formatted  Formatted  Formatted: German (Germany)  Formatted  Formatted: German (Germany)  Formatted  Formatted  Formatted  Formatted  Formatted  Formatted  Formatted: German (Germany)	
1110 1115 1120	Sun, L., Xie, Z., and Zhao, J.; A 3,000-year record of penguin populations, Nature, 407, 858-858, 10.1038/35038163, 2000. Tatur, A., Myrcha, A., and Niegodzisz, J.; Formation of abandoned penguin rookery ecosystems in the maritime Antarctic, Polar Biology, 17, 405-417, 10.1007/s003000050135, 1997.  Taylor, F., Whitehead, J., and Domack, Ε.; Holocene paleoclimate change in the Antarctic Peninsula: evidence from the diatom, sedimentary and geochemical record, Mar. Micropaleontol., 41, 25-43, https://doi.org/10.1016/S0377-8398(00)00049-9, 2001.  Ter Braak, C. and Smilauer, P.; Canoco for Windows version 4.5, Biometris—Plant Research International, Wageningen, 2002.  Totten, R. L., Anderson, J. B., Fernandez, R., and Wellner, J. S.; Marine record of Holocene climate, ocean, and cryosphere interactions: Herbert Sound, James Ross Island, Antarctica, Quaternary Science Reviews, 129, 239-259, https://doi.org/10.1016/j.quascirev.2015.09.009, 2015.  Turner, J., Guarino, M. V., Arnatt, J., Jena, B., Marshall, G. J., Phillips, T., Bajish, C. C., Clem, K., Wang, Z., Andersson, T., Murphy, E. J., and Cavanagh, R.; Recent Decrease of Summer Sea Ice in the Weddell Sea, Antarctica, Geophysical Research Letters, 47, e2020GL087127, https://doi.org/10.1029/2020GL087127, 2020.  Valenzuela, L. O., Rowntree, V. J., Sironi, M., and Seger, J.; Stable isotopes (δ15N, δ13C, δ13C), δ13C, δ1		Formatted  Formatted: German (Germany)  Formatted  Formatted  Formatted: German (Germany)  Formatted  Formatted  Formatted: German (Germany)  Formatted  Formatted  Formatted	
1110 1115 1120	Sun, L., Xie, Z., and Zhao, J.; A 3,000-year record of penguin populations, Nature, 407, 858-858, 10.1038/35038163, 2000. Tatur, A., Myrcha, A., and Niegodzisz, J.; Formation of abandoned penguin rookery ecosystems in the maritime Antarctic, Polar Biology, 17, 405-417, 10.1007/s003000050135, 1997.  Taylor, F., Whitehead, J., and Domack, E.; Holocene paleoclimate change in the Antarctic Peninsula: evidence from the diatom, sedimentary and geochemical record, Mar. Micropaleontol., 41, 25-43, https://doi.org/10.1016/S0377-8398(00)00049-9, 2001.  Ter Braak, C. and Smilauer, P.; Canoco for Windows version 4.5, Biometris—Plant Research International, Wageningen, 2002.  Totten, R. L., Anderson, J. B., Fernandez, R., and Wellner, J. S.; Marine record of Holocene climate, ocean, and cryosphere interactions: Herbert Sound, James Ross Island, Antarctica, Quaternary Science Reviews, 129, 239-259, https://doi.org/10.1016/j.quascirev.2015.09.009, 2015.  Turner, J., Guarino, M. V., Arnatt, J., Jena, B., Marshall, G. J., Phillips, T., Bajish, C. C., Clem, K., Wang, Z., Andersson, T., Murphy, E. J., and Cavanagh, R.; Recent Decrease of Summer Sea Ice in the Weddell Sea, Antarctica, Geophysical Research Letters, 47, e2020GL087127, https://doi.org/10.1029/2020GL087127, 2020.  Valenzuela, L. O., Rowntree, V. J., Sironi, M., and Seger, J.; Stable isotopes (815N, 813C, 834S) in skin reveal diverse food sources used by southern right whales Eubalaena australis, Marine Ecology Progress Series, 603, 243-255, 2018.  van den Berg, G. L., Vermeulen, E., Valenzuela, L. O., Bérubé, M., Ganswindt, A., Gröcke, D. R., Hall, G., Hulva, P., Neveceralova, P., Palsbøll, P. J., and Carroll, E. L.; Decadal shift in foraging strategy of a migratory southern ocean predator, Global Change Biology, 27, 1052-1067, https://doi.org/10.1111/gcb.15465, 2021.  Verleyen, E., Hodgson, D. A., Sabbe, K., Cremer, H., Emslie, S. D., Gibson, J., Hall, B., Imura, S., Kudoh, S., Marshall, G. J., McMinn, A., Melles, M., Newman, L., Roberts, D., Roberts, S. J., Singh, S		Formatted  Formatted: German (Germany)  Formatted  Formatted  Formatted: German (Germany)  Formatted  Formatted: German (Germany)  Formatted  Formatted  Formatted  Formatted  Formatted  Formatted  Formatted: German (Germany)	

Vernet, M., Geibert, W., Hoppema, M., Brown, P. J., Haas, C., Hellmer, H. H., Jokat, W., Jullion, L., Mazloff, M., Bakker, D. C. E., Brearley, J. A., Croot, P., Hattermann, T., Hauck, J., Hillenbrand, C.-D., Hoppe, C. J. M., Huhn, O., Koch, B. P., Lechtenfeld, O. J., Meredith, M. P., Naveira Garabato, A. C., Nöthig, E.-M., Peeken, I., Rutgers van der Loeff, M. M., Schmidtko, S., Schröder, M., Strass, V. H., Torres-Valdés, S., and Verdy, A., The Weddell Gyre, Southern Ocean: Present Knowledge and Future Challenges, Reviews of Geophysics, 57, 623-708, https://doi.org/10.1029/2018RG000604, 2019.
von Berg, L., Prend, C. J., Campbell, E. C., Mazloff, M. R., Talley, L. D., and Gille, S. T. Weddell Sea Phytoplankton Blooms

135 Modulated by Sea Ice Variability and Polynya Formation Geophysical Research Letters 47 e2020GL087954, 2020.
Vorrath, M. E., Müller, J., Cárdenas, P., Opel, T., Mieruch, S., Esper, O., Lembke-Jene, L., Etourneau, J., Vieth-Hillebrand, A., Lahajnar, N., Lange, C. B., Leventer, A., Evangelinos, D., Escutia, C., and Mollenhauer, G.: Deglacial and Holocene seaice and climate dynamics in the Bransfield Strait, northern Antarctic Peninsula, Clim. Past, 19, 1061-1079, 10.5194/cp-19-1061-2023, 2023.

Wainright, S. C., Haney, J. C., Kerr, C., Golovkin, A. N., and Flint, M. V.: Utilization of nitrogen derived from seabird guano by terrestrial and marine plants at St. Paul, Pribilof Islands, Bering Sea, Alaska, Marine Biology, 131, 63-71, 10.1007/s002270050297, 1998.

Wakefield, E. D., McClymont, E. L., Descamps, S., Grecian, W. J., Honan, E. M., Rix, A. S., Robert, H., Sandøy Bråthen, V., and Phillips, R. A.: Variability in foraging ranges of snow petrels and implications for breeding distribution and use of sto mach-

145 oil deposits as proxies for paleoclimate, bioRxiv [preprint], 2025.2006.2006.658237, 10.1101/2025.06.06.658237, 2025.
Wang, J., Massonnet, F., Goosse, H., Luo, H., Barthélemy, A., and Yang, Q.; Synergistic atmosphere-ocean-ice influences have driven the 2023 all-time Antarctic sea-ice record low, Communications Earth & Environment, 5, 415, 10.1038/s43247-024-01523-3, 2024.

Warham, J., Watts, R., and Dainty, R. J.: The composition, energy content and function of the stomach oils of petrels (order, procellariiformes), Journal of Experimental Marine Biology and Ecology, 23, 1-13, https://doi.org/10.1016/0022-0981(76)90081-2, 1976.

Watts, R. and Warham, J<sub>7.2</sub>Structure of some intact lipids of petrel stomach oils Lipids 11 423-429, 10.1007/BF02532831

Wickham, H., Averick, M., Bryan, J., Chang, W., McGowan, L. D. A., François, R., Grolemund, G., Hayes, A., Henry, L., and Hester, J.:, Welcome to the Tidyverse, Journal of Open Source Software, 4, 1686, 2019.

Xavier, J. C., Raymond, B., Jones, D. C., and Griffiths, H.: Biogeography of Cephalopods in the Southern Ocean Using Habitat Suitability Prediction Models, Ecosystems, 19, 220-247, 10.1007/s10021-015-9926-1, 2016.

Xiao, W., Esper, O., and Gersonde, R.: Last Glacial - Holocene climate variability in the Atlantic sector of the Southern Ocean, Quaternary Science Reviews, 135, 115-137, 2016.

160 Zhou, L., Heuzé, C., and Mohrmann, M. Early Winter Triggering of the Maud Rise Polynya Geophysical Research Letters 49 e2021GL096246, 2022https://doi.org/10.1016/j.quascirev.2016.01.023, 2016.

Formatted: Germany) Formatted: Germany) Formatted: Font: Not Italic, German (Germany) Formatted: Germany) Formatted: Germany) Formatted: German (Germany) Formatted: Germany) Formatted: Germany) Formatted: Germany) Formatted: Font: Not Italic, German (Germany) Formatted: Germany) Formatted: Germany) Formatted: German (Germany) Formatted: German (Germany) Formatted: Germany) Formatted: Font: Not Italic, German (Germany) Formatted: German (Germany) Formatted: Germany) Formatted: Germany) Formatted: Germany) Formatted: German (Germany) Formatted: Font: Not Italic, German (Germany) Formatted: Germany) Formatted: Germany) Formatted: Germany) Formatted: Germany) Formatted: Germany) Formatted: Font: Not Italic, German (Germany) Formatted: Germany) Formatted: German (Germany) Formatted: Germany) Formatted: Germany) Formatted: Font: Not Italic, German (Germany) Formatted: Germany) Formatted: Germany)

Formatted: German (Germany)
Formatted: Font: Not Italic
Formatted: German (Germany)